



Research article

Treatment of microglia with Anti-PrP monoclonal antibodies induces neuronal apoptosis *in vitro*

Utpal Kumar Adhikari^a, Elif Sakiz^a, Umma Habiba^a, Meena Mikhael^a, Matteo Senesi^{b,c},
Monique Antoinette David^a, Gilles J. Guillemain^d, Lezanne Ooi^{e,f}, Tim Karl^{a,g,h},
Steven Collins^{b,c}, Mourad Tayebi^{a,*}

^a School of Medicine, Western Sydney University, Campbelltown, NSW, Australia

^b Australian National Creutzfeldt-Jakob Disease Registry (ANCJDR), The Florey Institute of Neuroscience and Mental Health, The University of Melbourne, Parkville, 3010, Australia

^c Department of Medicine, Royal Melbourne Hospital, The University of Melbourne, Parkville, 3010, Australia

^d Department of Biomedical Sciences, Faculty of Medicine and Health Sciences, Macquarie University, NSW, Australia

^e Illawarra Health and Medical Research Institute, Wollongong, 2522, NSW, Australia

^f School of Chemistry and Molecular Bioscience, University of Wollongong, Wollongong, 2522, NSW, Australia

^g Neuroscience Research Australia (NeuRA), NSW, Australia

^h School of Medical Sciences, University of New South Wales, NSW, Australia

HIGHLIGHTS

- Antibody cross-linking neuronal PrPC induces apoptosis.
- Antibody cross-linking microglial PrPC induces neuronal apoptosis.
- Different apoptotic pathways were triggered by specific anti-PrP antibody treatments.

ARTICLE INFO

Keywords:

Anti-PrP antibodies
Apoptosis
Cellular prion protein
Microglia
Neuroblastoma cell line (N2a)
Microglia cell line (N11)
Primary neuronal cells

ABSTRACT

Previous reports highlighted the neurotoxic effects caused by some motif-specific anti-PrP^C antibodies *in vivo* and *in vitro*. In the current study, we investigated the detailed alterations of the proteome with liquid chromatography–mass spectrometry following direct application of anti-PrP^C antibodies on mouse neuroblastoma cells (N2a) and mouse primary neuronal (MPN) cells or by cross-linking microglial PrP^C with anti-PrP^C antibodies prior to co-culture with the N2a/MPN cells. Here, we identified 4 (3 upregulated and 1 downregulated) and 17 (11 upregulated and 6 downregulated) neuronal apoptosis-related proteins following treatment of the N2a and N11 cell lines respectively when compared with untreated cells. In contrast, we identified 1 (upregulated) and 4 (2 upregulated and 2 downregulated) neuronal apoptosis-related proteins following treatment of MPN cells and N11 when compared with untreated cells. Furthermore, we also identified 3 (2 upregulated and 1 downregulated) and 2 (1 upregulated and 1 downregulated) neuronal apoptosis-related related proteins following treatment of MPN cells and N11 when compared to treatment with an anti-PrP antibody that lacks binding specificity for mouse PrP. The apoptotic effect of the anti-PrP antibodies was confirmed with flow cytometry following labelling of Annexin V-FITC. The toxic effects of the anti-PrP antibodies was more intense when antibody-treated N11 were co-cultured with the N2a and the identified apoptosis proteome was shown to be part of the PrP^C-interactome. Our observations provide a new insight into the prominent role played by microglia in causing neurotoxic effects following treatment with anti-PrP^C antibodies and might be relevant to explain the antibody mediated toxicity observed in other related neurodegenerative diseases such as Alzheimer.

* Corresponding author.

E-mail address: m.tayebi@westernsydney.edu.au (M. Tayebi).

1. Introduction

Prion diseases are a group of fatal neurodegenerative diseases characterized by the conversion of the α -helices-rich cellular prion protein, PrP^C and deposition in the central nervous system (CNS) of humans and animals of a disease specific isoform, PrP^{Sc} that is rich in β -sheet structure and partially proteinase-resistant (Prusiner and DeArmond, 1994; Tayebi and Hawke, 2006). The majority of PrP molecules carry bi-, tri- and tetra-antennary neutral and N-linked sialylated oligosaccharides at two sites (Endo et al., 1989; Haraguchi et al., 1989). A disulfide bond links the only two cysteines in the mature prion protein (Turk et al., 1988).

Several drugs have been tested for interaction with PrP^{Sc} and its accumulation, including Polyaniions (Ehlers and Diring, 1984), Iodo-doxorubicin, Tetracycline (Forloni et al., 2002) Congo red (Caughey and Raymond, 1993), β -sheet breakers (Soto et al., 2000), Polyene antibiotics (Adjou et al., 2000), Chlorpromazine and Quinacrine (Korth et al., 2001). Only amphotericin analogue MS8209 has had an appreciable effect on the disease course (Adjou et al., 1995, 1996). Otherwise, many of these drugs suppress prion replication *in vitro* but fail to show significant efficacy *in vivo*. Alternative treatment strategies for prions include antibody-mediated therapy which appears to be one of the most promising approaches (Bardelli et al., 2018; Heppner et al., 2001; Schwarz et al., 2003; Sigurdsson et al., 2002; White et al., 2003). One of the earliest reports that established the proof-of-concept for *in vivo* prion immunotherapy demonstrated that antibodies for both PrP conformers were able to prevent prion disease onset (White et al., 2003). However, some of these anti-PrP antibodies led to neuronal apoptosis *in vivo* (Jones et al., 2010; Solforosi et al., 2004), Fyn activation (Mouillet-Richard et al., 2000) and modulation of calcium-dependent protein kinase C in mice (Mazzoni et al., 2005) following cross-linking PrP^C. Moreover, it was also demonstrated that treatment of neuronal cells with therapeutic anti-PrP antibodies caused overexpression of apolipoprotein E, activation of cytoplasmic phospholipase A2 and production of prostaglandin (Tayebi et al., 2010). This report by Tayebi and colleagues demonstrated that the toxicity was achieved via binding an anti-PrP antibody to the N-terminal region of PrP^C, while an antibody that bound an epitope located on the C-terminal domain of PrP^C was innocuous and failed to cause apoptosis (Tayebi et al., 2010). Interestingly, both the N- and C-terminal antibodies were subsequently shown to be safe and did not lead to hippocampal neuronal apoptosis following their intracranial administration to mice (Klöhn et al., 2012). Nevertheless, a later study by Reimann and colleagues disputed these findings by demonstrating that the anti-PrP antibody with specific binding to the N-terminal side of PrP^C led to neurotoxicity (Reimann et al., 2016), confirming the epitope-specific neurotoxicity following cross-linking PrP^C (Bardelli et al., 2018; Tayebi et al., 2010).

Microglial activation can be triggered by various factors which in turn contributes to neurodegeneration (Aguzzi and Falsig, 2012). Gliosis is a well-established hallmark of most neurodegenerative disorders, including prion diseases (Aguzzi and Zhu, 2017; Baker et al., 2002; Monzón et al., 2018). Microglia-related molecules, such as cytokines (Schultz et al., 2004), toll-like receptors (TLRs) (Sethi et al., 2002), inflammatory regulators (Mok et al., 2007), chemokines (Felton et al., 2005), complement systems (Lv et al., 2015), and phagocytosis mediators (Hanayama et al., 2002; N'Diaye et al., 2009; Takahashi et al., 2005) are involved in the pathogenesis of prion diseases (Aguzzi and Zhu, 2017). It was previously reported that the cytotoxic effects on primary cells following treatment with a PrP peptide were dependent on microglia activation, suggesting that these are important mediators for inducing neuronal death (Brown et al., 1996). In this study, we used a set of anti-PrP antibodies, including ICSM (Beringue et al., 2003), SAF (Demart et al., 1999; Féraud et al., 2005) and POM (Polymenidou et al., 2008) that bind to either the globular domain (GD) or flexible tail (FT) of PrP^C (Table 1 and Figure 1) and treated a neuroblastoma (N2a) (Klebe, 1969), mouse primary neuron (MPN), and a microglial (N11) cell line (Righi et al., 1989) to investigate the molecular mechanisms underlying

antibody-induced toxicity. Mass spectrometry analysis was applied to detect a shift in the cell proteome, to identify apoptosis related proteins and to characterize possible pathways leading to apoptosis post-antibody treatment.

We showed that direct application of anti-PrP antibodies on N2a can trigger apoptosis and we identified 4 (3 upregulated and 1 downregulated) apoptosis-related proteins. Co-culture of N2a with antibody treated N11 led to a more substantial disturbance of the proteome and we identified 17 (11 upregulated and 6 downregulated) apoptosis related proteins. Moreover, we also identified 1 (upregulated) and 4 (2 upregulated and 2 downregulated) neuronal apoptosis-related proteins following direct treatment of mouse primary neuronal (MPN) cells (Haigh et al., 2011) or co-culture of antibody-treated N11 with MPN cells when compared with untreated cells. Similarly, 3 (2 upregulated and 1 downregulated) and 2 (1 upregulated and 1 downregulated) neuronal apoptosis-related proteins were identified when compared with control 3F4 anti-PrP antibody (Kasczak et al., 1987) treatment.

This study not only confirms the toxic effects of anti-PrP antibodies with binding specificity to the GD of PrP^C but importantly, emphasizes the important role played by microglia in triggering apoptosis.

2. Materials and methods

2.1. Cell lines and mouse primary cell lines

N2a Cell Line: N2a is an adherent cell and its morphology is neuronal-like and resembles amoeboid stem cells. N2a cells produce large quantities of microtubular protein which is believed to play a role in a contractile system responsible for axoplasmic flow in nerve cells. This cell line was used extensively as an *in vitro* model to study prion infection and antibody toxicity (Enari et al., 2001; Jones et al., 2010; Pankiewicz et al., 2006; Wu et al., 2017).

N11 Cell Line: The N11 cell line was produced by Righi et al. from embryonic brain primary cell cultures by immortalizing microglial cells with oncogenic retroviruses (Righi et al., 1989). The viruses used were new recombinants (termed 3RV) carrying the v-myc or v-mil oncogenes of the avian retrovirus MH2. N11 is able to produce several cytokines, namely interleukin 1 (IL 1), interleukin 6 (IL 6) and tumour necrosis factor α (TNF- α). N11 exhibits the phenotype for microglial cells since they are F4/80', FcR', Mac-1' positive and do not express astroglial, bipotential glial precursor or oligodendroglial markers (GFAP-, A2B5- and Gal-C-) (Righi et al., 1989).

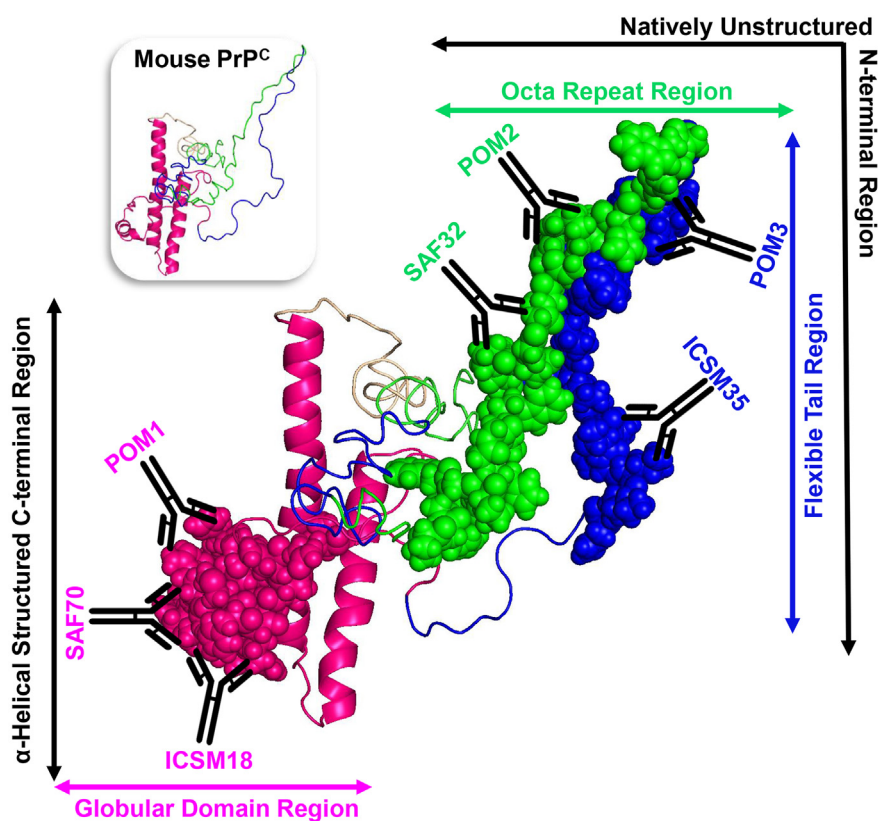
The mice primary neuronal (MPN) cells were produced from eight week-old wild-type (WT) mice (C57BL/6 x SV129 background) (Haigh et al., 2011). Initially, neuronal stem cells (NSC) used in this study for differentiation into mouse primary neurons (MPN) were harvested from the sub ventricular zone (SVZ) of the whole brain of WT mice as described (Haigh et al., 2011).

2.2. Treatment of mouse neuroblastoma and microglia cell lines with Anti-PrP antibodies

We used mouse neuroblastoma (N2a) (American Type Culture Collection, ATCC, USA) (Klebe, 1969) and microglia (N11) (Righi et al., 1989) cell lines to investigate the neurotoxic effect of anti-PrP antibodies. The N2a cells were used to assess toxicity following direct application of anti-PrP antibodies (DAT). The N11 cells, initially treated with anti-PrP antibodies, were used to assess their toxic effects on N2a cells following direct co-culture (DMT) or after separating the N11 antibody treated and N2a cells by a tissue culture insert (IMT). Both N2a and N11 cells were grown in complete medium [Dulbecco's Modified Eagle Medium (DMEM) (Thermo Fisher Scientific, Australia), 10% fetal bovine serum (FBS) (Gibco, Fisher Scientific, Australia), and 1% Penicillin-streptomycin (Sigma, USA)] at 37 °C in 5% CO₂. For N2a differentiation, cells were initially cultured for 24 h in complete media then cultured in complete media containing 2% serum and 20 μ M retinoic acid

Table 1. Properties of the different anti-PrP antibodies used in this study.

| Antibody | Isotype | Immunogen | Adjuvant/Protein Carrier | Host Immunised Mouse Strain | Epitope Position | Epitope position in Structure | References |
|----------|---------|--|--------------------------|---|----------------------------------|-------------------------------|---------------------------|
| ICSM 18 | IgG1 | Human (α PrP91-231) | CFA and IFA | FVB/N Prnp ^{0/0} mice | 146–159 | Globular domain | Beringue et al. (2003) |
| ICSM 35 | IgG2b | Human ($r\beta$ PrP91-231) | CFA and IFA | FVB/N Prnp ^{0/0} mice | 91–110 | Flexible tail region | Beringue et al. (2003) |
| SAF 32 | IgG2b | SAF preparation from infected Syrian hamster brain (β) | KLH and CFA | back-footpads of Biozzi mice (Biozzi ABH) (PrP ^{0/0}) | 59–89 | Octa repeat region | Féraudet et al. (2005) |
| SAF70 | IgG2b | SAF preparation from infected Syrian hamster brain (β) | KLH and CFA | back-footpads of Biozzi mice (Biozzi ABH) (PrP ^{0/0}) | 142–160 | Globular domain | Demart et al. (1999) |
| POM1 | IgG1 | Mouse (α PrP23-231) | CFA | Prnp ^{0/0} mice | H1 (138–147) H3 (204/208/212) | Globular domain | Polymenidou et al. (2008) |
| POM2 | IgG1 | Mouse (α PrP23-231) | CFA | Prnp ^{0/0} mice | 57–88 | Octa repeat region | Polymenidou et al. (2008) |
| POM3 | IgG1 | Mouse (α PrP23-231) | CFA | Prnp ^{0/0} mice | 95–100 | Flexible tail region | Polymenidou et al. (2008) |

**Figure 1.** Schematic representation of the binding sites of different anti-PrP antibodies on the different regions of the mouse major prion protein.

for 48 h N2a cells were then washed and recultured in complete media containing 2% serum and 10 ng/ml BDNF for 24 h prior to use for the treatment studies.

2.2.1. Direct antibody treatment (DAT)

N2a cells were plated on a 24 well plates (Falcon, Becton. Dickinson, Australia) at 200,000 cells/well for 48 h in tissue culture medium and kept in a tissue culture incubator at 37 °C and 5% CO₂ until optimum growth and adhesion to the surface of the plates were observed. The medium was changed daily. After 48 h, 3µg of different anti-PrP antibodies ICSM18 (Beringue et al., 2003), ICSM35 (Beringue et al., 2003), POM1 (Polymenidou et al., 2008), POM2 (Polymenidou et al., 2008),

POM3 (Polymenidou et al., 2008), SAF32 (Féraudet et al., 2005), or SAF70 (Demart et al., 1999) were added daily to the N2a cultures for 3 days. On day 5, N2a cells were removed from the plates and centrifuged at 149xg (800 rpm) for 5 min. The cells were then lysed with NP-40 lysis buffer (150mM NaCl, 1.0% Nonidet P-40 and Triton X-100, 50 mM Tris-Cl, adjust P^H to 7.4) with addition of AEBSF protease inhibitor (Sigma, USA) and stored at –80 °C until further use.

2.2.2. Direct microglia treatment (DMT)

The N11 cells were plated and cultured on a 24 well plates at 200,000 cells/well for 48 h in culture medium (DMEM medium, 10% FBS, and 1% Penicillin-streptomycin) and incubated at 37 °C in 5% CO₂. N11 cells

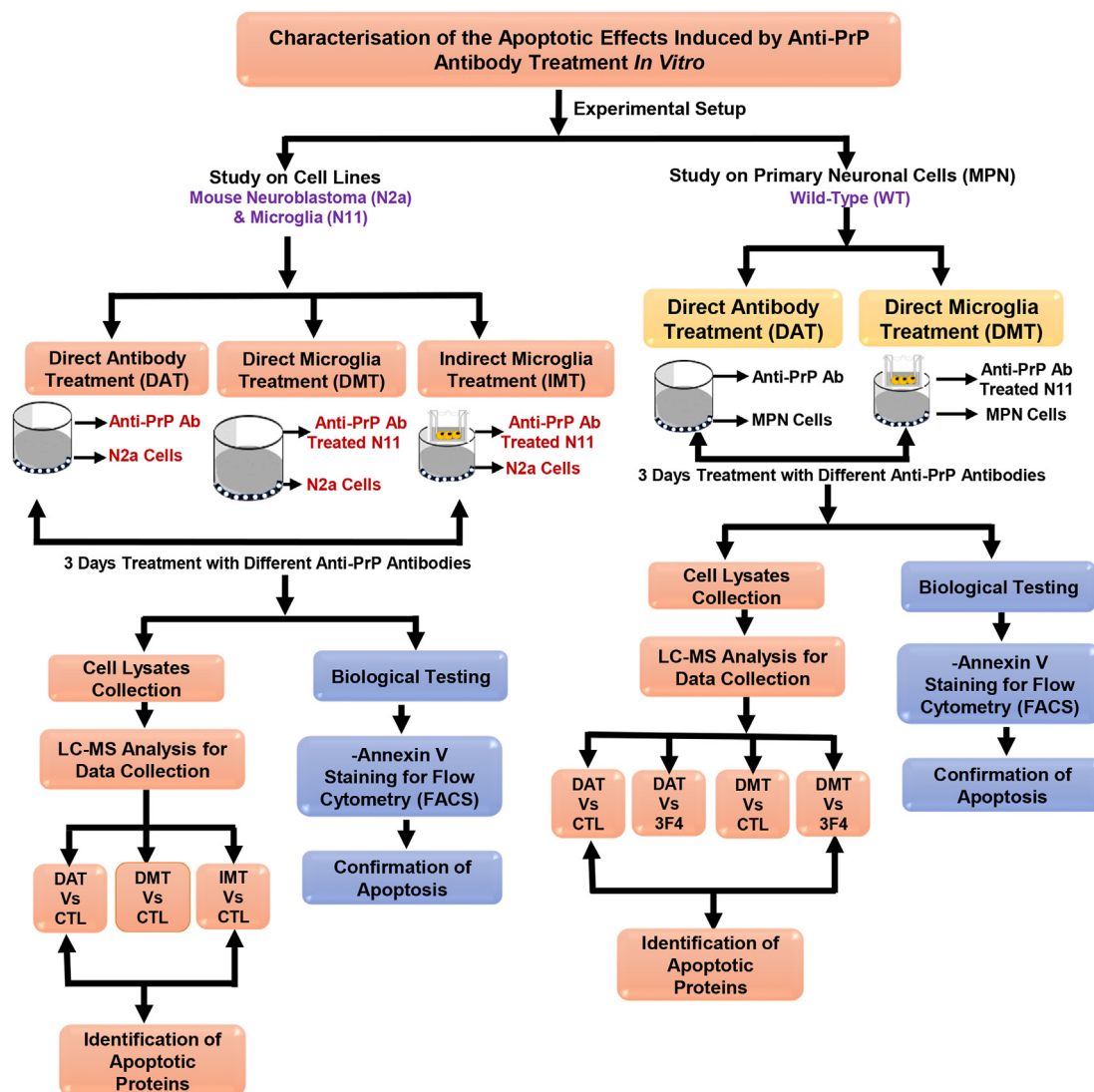


Figure 2. Overall methodology for the identification of apoptotic proteins following antibody treatment and LC-MS analysis.

were then treated with $3\mu\text{g}$ of different anti-PrP antibodies as above daily for 3 days. The antibody treated N11 cells were detached via trypsinization and centrifuged at $149\times g$ (800 rpm) for 5 min before co-culturing with confluent N2a cells for 3 days. Finally, the N2a/antibody-treated N11 co-culture was centrifuged at $149\times g$ (800 rpm) for 5 min and the pellet was lysed with NP-40 lysis buffer with addition of AEBSF protease inhibitor then stored at -80°C until further use.

2.2.3. Indirect microglia treatment (IMT)

In order to verify whether the potential toxic effect is caused by molecules released from N11 cells following treatment with anti-PrP antibodies, the N11 cells were plated and cultured on tissue culture inserts (Nunc™ Polycarbonate Cell Culture Inserts, 0.4-micron pore size) in 24 well plate at 200,000 cells/well for 48 h. The N11 cells were treated daily with $3\mu\text{g}$ of different anti-PrP antibodies as above. The tissue culture inserts containing antibody treated N11 cells were transferred to 24 well tissue culture plate containing confluent N2a cells and left for 3 days. Finally, the N2a cells were removed from the wells and centrifuged at $149\times g$ (800 rpm) for 5 min and lysed with NP-40 lysis buffer and AEBSF protease inhibitor before storing at -80°C until further use.

2.3. Treatment of mouse primary neuronal cells and microglia cell line with Anti-PrP antibodies

2.3.1. Direct antibody treatment (DAT) of primary neuronal cells

The WT mouse neuronal stem cells (NSC) were plated in 24 well plate at 50,000 cells/well in mice NeuroCult™ Differentiation kit (Stem Cell Technologies, Canada) and incubated at 37°C in 5% CO_2 for 7 days. The NSC were differentiated into mouse primary neuron (MPN) after 7 days which was checked by neuronal markers, NeuN and Nurr1. The cells were then treated daily with $1\mu\text{g}$ of ICSM18, ICSM35 (Beringue et al., 2003) or 3F4 (Sigma-Aldrich, Australia) for 3 days. Cells were trypsin-removed from the plates, centrifuged at $149\times g$ (800 rpm) for 5 min and lysed with NP-40 lysis buffer (150mM NaCl, 1.0% Nonidet P-40 and Triton X-100, 50 mM Tris-Cl, adjust pH to 7.4) with addition of AEBSF protease inhibitor (Sigma, USA) and stored at -80°C until further use.

2.3.2. Direct microglia treatment (DMT) of primary neuronal cells

The N11 cells were plated and cultured on a 24 well plate at 50,000 cells/well for 24 h in culture medium (DMEM medium, 10% FBS, and 1%

Penicillin-streptomycin) and incubated at 37 °C in 5% CO₂. N11 cells were then treated with 1 µg of ICSM18, ICSM35 or 3F4 antibody as above. The antibody treated N11 cells were centrifuged at 149xg (800 rpm) for 5 min before co-culturing with confluent WT MPN cells for 3 days. Finally, the WT MPN cells and antibody treated N11 co-culture was centrifuged at 149xg (800 rpm) for 5 min and the pellet was lysed with NP-40 lysis buffer with addition of AEBSF protease inhibitor then stored at –80 °C until further use.

2.3.3. Immunofluorescence analysis of primary neuronal cells

Immunofluorescence analysis was performed to confirm whether the mouse neuronal stem cells have been fully differentiated to become mature neurons expressing PrP^C. Cover slips were sterilized by immersing in 70% ethanol followed by washing in 100% ethanol, rinsing in autoclaved water, and finally washing with RPMI. The coverslips were then coated with Matrigel (Sigma-Aldrich, USA) solution. The fully differentiated WT MPN cells were transferred to a new 24 well plates

Table 2. Properties of the identified all proteins including apoptotic proteins following direct antibody treatment (DAT) of the neuroblastoma cell line. The properties were identified by Progenesis Software after the LC-MS analysis.

| Accession | Protein Name | Gene ID | Subcellular location | Unique peptides | Confidence score | Anova (p) | Max fold change | Highest Mean | Lowest Mean |
|------------|--|---------|--|-----------------|------------------|-------------|-----------------|--------------------|--------------------|
| A0A2I3BP10 | Coiled-coil domain-containing protein 187 | Ccdc187 | Cytoskeleton | 2 | 55.9 | 0.04328225 | 33.2 | Control | Antibody Treatment |
| B2RUM8 | RNA helicase | Ddx18 | Nucleus | 4 | 57.5 | 0.00837738 | 20 | Control | Antibody Treatment |
| P19426 | Negative elongation factor E | Nelfe | Nucleus | 5 | 117 | 0.0036431 | 12.3 | Control | Antibody Treatment |
| Q497U2 | Pcnt protein (Fragment) | Pcnt | Cytoskeleton, Cytosol | 2 | 107 | 0.02199705 | 20.3 | Control | Antibody Treatment |
| Q05816 | Fatty acid-binding protein 5 | Fabp5 | Nucleus | 3 | 260 | 0.01718987 | 16 | Control | Antibody Treatment |
| A0A0N4SVL0 | Eukaryotic translation initiation factor 4 gamma 3 | Eif4g3 | cytosol | 3 | 88.3 | 0.00489254 | 14.1 | Antibody Treatment | Control |
| A0A2R8VHP3 | Predicted pseudogene 5478 | Gm5478 | Cytoskeleton | 2 | 91.5 | 0.00393282 | 267 | Antibody Treatment | Control |
| A2A8L5 | Receptor-type tyrosine-protein phosphatase F | Ptprf | plasma membrane | 5 | 102 | 0.00607666 | 11.9 | Antibody Treatment | Control |
| A2RSV8 | Cytochrome c oxidase subunit IV isoform | Cox4i1 | mitochondrion | 2 | 60.5 | 0.00229063 | 17.9 | Antibody Treatment | Control |
| A2RSY1 | KAT8 regulatory NSL complex subunit 3 | Kansl3 | Nucleus | 3 | 74.2 | 0.03078433 | 13.7 | Antibody Treatment | Control |
| A4FUV6 | Met protein (Fragment) | Met | plasma membrane | 7 | 130 | 0.00315318 | 23.4 | Antibody Treatment | Control |
| A7E215 | Rps6ka3 protein (Fragment) | Rps6ka3 | Nucleus, Cytosol | 3 | 42.8 | 0.03518287 | 18 | Antibody Treatment | Control |
| B1AZR7 | Protocadherin 11 X-linked | Pcdh11x | Plasma membrane | 4 | 60.8 | 0.00666053 | 11.7 | Antibody Treatment | Control |
| E9QKD1 | Nucleolar protein 8 | Nol8 | Nucleus | 2 | 74.5 | 0.04856417 | 201 | Antibody Treatment | Control |
| H7BX49 | WD repeat-containing protein 90 | Wdr90 | Cytoskeleton | 3 | 73.6 | 0.04129529 | 16.1 | Antibody Treatment | Control |
| Q3TW28 | Uncharacterized protein | Tpp2 | Nucleus, Cytosol | 9 | 171 | 0.00407148 | 111 | Antibody Treatment | Control |
| B1GX81 | PAK3cb protein | Pak3 | Cytosol, Plasma membrane | 3 | 37.7 | 0.022568968 | 11.2 | Antibody Treatment | Control |
| Q3UBP6 | Uncharacterized protein | Actb | Extracellular, Cytoskeleton, Nucleus | 3 | 802 | 0.01880576 | 12.3 | Antibody Treatment | Control |
| Q3UR03 | Myomegalin (Fragment) | Pde4dip | Cytoskeleton, Nucleus, golgi apparatus | 3 | 49.1 | 0.02084224 | 29.9 | Antibody Treatment | Control |
| Q5U430 | E3 ubiquitin-protein ligase | Ubr3 | plasma membrane | 3 | 53.5 | 0.00548724 | 65.4 | Antibody Treatment | Control |
| Q6PDI5 | Proteasome adapter and scaffold protein ECM29 | Ecpas | Cytoskeleton, Nucleus, Endoplasmic reticulum, Endosome | 6 | 142 | 0.00749419 | 11.1 | Antibody Treatment | Control |
| Q8K442 | ATP-binding cassette sub-family A member 8-A | Abca8a | Plasma membrane | 2 | 60 | 0.00447174 | 12.7 | Antibody Treatment | Control |
| Q9WUM5 | Succinate-CoA ligase [ADP/GDP-forming] subunit alpha_mitochondrial | Suclg1 | Mitochondrion | 4 | 68.1 | 0.04593013 | 17.1 | Antibody Treatment | Control |
| Q80XC6 | Nuclear exosome regulator NRDE2 | Nrde2 | Nucleus | 2 | 46.5 | 0.04874164 | 28.8 | Antibody Treatment | Control |
| Q99JW2 | Aminoacylase-1 | Acy1 | Extracellular, Cytosol | 2 | 62.7 | 0.02111784 | Infinite | Antibody Treatment | Control |
| Q499M4 | Tigger transposable element derived 5 | Tigd5 | Nucleus | 2 | 45.2 | 0.01042085 | 10.7 | Antibody Treatment | Control |
| Q02819 | Nucleobindin-1 | Nucb1 | Extracellular, Endoplasmic reticulum | 4 | 52 | 0.04447922 | 33.1 | Antibody Treatment | Control |

containing cold PBS. The coverslips were rinsed two times in cold PBS followed by addition of 300µL of 4% paraformaldehyde for 20 min at room temperature. The coverslips were then washed x3 with in cold PBS. 0.01% Triton was added to the coverslips and left to incubate for 1 min, followed by washing then addition of 2% BSA for 20 min. Primary mouse anti-NeuN antibody (1:500) (MerckMillipore, Australia), rabbit Anti-Nurr1 (1:500) (Life Technology, Australia), and ICSM18 antibody (1:1000) was added for 1 h at room temperature followed by secondary anti-mouse IgG (H + L)-Texas Red antibody (Sigma-Aldrich, USA) (1:500 dilution) and goat anti-rabbit IgG (H + L)-FITC antibody (1:500 dilution) (Sigma-Aldrich, USA) for 1 h at room temperature. The coverslips were washed with PBS x3 and finally mounted on glass slides using VECTA-SHIELD HardSet Antifade Mounting Medium with DAPI (Vector Laboratories, CA, USA) in aqueous mounting media (Agilent Technologies, CA, USA) (1:3 ratio) and sealed with clear nail polish to prevent dehydration.

2.3.4. Flow cytometry analysis

For DAT and DMT, cell lines and MPN cells were treated as above. Some cells were also treated with 500µM H₂O₂ for 30 min in a tissue culture incubator at 37 °C in 5% CO₂. Following treatment with antibodies or H₂O₂, cells were scrapped and kept in the incubator for 30 min for membrane recovery. The cells were then transferred into FACS tubes (Stem Cell Technologies, Australia) and centrifuged for 5 min at 4 °C at 186xg (1000 rpm). Cells were washed with cold PBS prior to addition of 100µL of 1x Annexin binding buffer (Invitogen, Australia). This was followed by adding 3µL of Alexa Fluor® 488 Annexin V (Invitogen, Australia) and 1µL of 100 µg/mL propidium iodide (PI) working solution (Invitogen, Australia) to each 100µL of cell suspension and incubated for 15 min at room temperature. 400µL 1X Annexin-binding buffer was added Flow cytometry analysis. Analysis was performed using MACS-Quant Analyzer (Miltenyi Biotec, Australia). Raw data was analysed on FlowJo software (version 10.7.1, LLC, Ashland, OR, USA).

2.4. Sample preparation for liquid chromatography-mass spectrometry

Following antibody treatment, the cells were lysed as above for use in Liquid Chromatography-Mass Spectrometry (LC-MS). For trypsin digestion, 100µL of protein sample (300 µg/mL cell lines or 170 µg/ml primary cells) of DAT, DMT and IMT were concentrated using Rotational Vacuum Concentrator (Martin Christ Gefrier-trocknungsanlagen GmbH, Germany). 6µL DTT (Roche Diagnostics Deutschland GmbH, Germany) (200 mM DTT in Tris buffer, p^H 7.8) was then added and the mixture was vortexed before addition of 30µL of 6M Urea into the sample then incubated for 1h at room temperature. 6µL iodoacetamide (Sigma-Aldrich, Australia) alkylating reagent (200mM iodoacetamide in Tris buffer, p^H 7.8) was then added, the sample mixture vortexed then followed by incubation for 1h at room temperature. The mixture was topped up with 225µL of distilled water before adding 5µL of trypsin (Promega Corporation, USA) solution and incubated overnight at 37 °C. Finally, the reaction was stopped, and the p^H of the solution adjusted to <6 with concentrated acetic acid.

After trypsin digestion, the solution was purified using Solid Phase Extraction (SPE) vacuum manifold (Waters Milford, Massachusetts, USA) then reconstituted in 15µL 0.1% formic acid, vortexed and kept for 30

min at 25 °C The solution was then vortexed and sonicated for 3 min then centrifuged at 14,000 rpm for 10 min before transferring into labelled glass vials.

2.5. Liquid chromatography-mass spectrometry analysis

The samples prepared above were carefully placed in a Waters Total Recovery chromatography sample vials for analysis. System specific cleaning protocol was run before loading the sample to avoid contamination in the system. LC-MS was performed using a Waters nanoAcquity UPLC equipped with a Waters nanoEase M/Z Peptide BEH C18 Column, 130Å, 1.7 µm 75 µm x 100 mm, thermostatted to 40 °C (Waters Corporation, USA). Briefly, solvent A consisted of ultrapure water (Milli-Q) plus 0.1% formic acid and solvent B consisted of LC-MS grade acetonitrile (Burdick and Jackson) plus 0.1% formic acid. Samples were injected onto a trapping column (Waters nanoEase M/Z Symmetry C18 Trap Column, 100A, 5 µm, 180 µm × 20mm) at 5µL/min at 99% Solvent A for 3 min before being eluted on the Analytical Column with a flowrate of 0.30µL/min. An initial solvent composition of 1% B was ramped to 85% B over 50 min. Injections of 1 µL were made from sample solutions stored at 4 °C.

Mass spectrometry was performed using a Waters SYNAPT G2-Si (HDMS) spectrometer fitted with a nano electrospray ionization source and operating in positive ion mode. Mass accuracy was maintained by infusing at 0.5 µL/min a lock spray solution of 1 pg/µL leucine enkephalin in 50% aqueous acetonitrile, plus 0.1% formic acid, calibrated against a sodium iodide solution. The capillary voltage was maintained at 3 kV, cone voltage at 30 V, source offset at 30 V, ion block temperature 80 °C, gas (N₂) flows: purge gas 20 L/h, cone gas 20 L/h. MassLynx Mass Spectrometry Software (Waters Corporation, USA) was used to process the data. Samples from 2 biological replicates were run three times in the LC-MS system and finally the collected data was processed against the mouse proteome using Uniprot database and analysed using Progenesis QI software (Waters Corporation, USA).

2.6. Functional analysis and protein-protein interaction prediction

Functional analysis of the final dataset of DAT, DMT and IMT was performed using DAVID Bioinformatics Resources 6.8 (<https://david.nci.crf.gov/>) (Huang et al., 2009; Jiao et al., 2012). DAVID is an enriched online unified biological knowledge base and analytic tools which thoroughly extract the biological meaning from the expansive gene or protein list (Huang et al., 2009). The interaction analysis among all the identified genes or proteins were achieved using STRING v11.0 (<http://string-db.org/>). This online platform is used as functional protein association networks which provides an in-depth assessment and integration of protein-protein interactions including both direct and indirect associations (Szklarczyk et al., 2015).

2.7. Classification of gene and gene enrichment analysis

The identified gene dataset was submitted to the online-based PANTHER classification system v14.0 (<http://www.pantherdb.org/>) for the classification of the identified genes based on the biological process, cellular components, molecular function, protein class, and signalling pathways (Mi et al., 2019). This is a wide-ranging system that helps

Table 3. Identification of antibody-specific apoptotic proteins following direct antibody treatment (DAT) of neuroblastoma cell lines.

| Accession ID | Gene ID | Effect of Anti-PrP Antibodies | | | | | | | | |
|--------------|---------|-------------------------------|-----|--------|-----|-------|-----|------|-----|---|
| | | ICSM18 | CTL | ICSM35 | CTL | SAF70 | CTL | POM1 | CTL | |
| Q497U2 | Pcnt | - | √ | - | - | - | - | - | - | - |
| A2A8L5 | Ptprf | - | - | - | - | - | - | - | - | - |
| A7E215 | Rps6ka3 | √ | - | - | - | - | - | - | - | - |
| B1GX81 | Pak3 | - | - | - | - | - | - | - | - | - |

(√) Upregulated and (-) Downregulated.

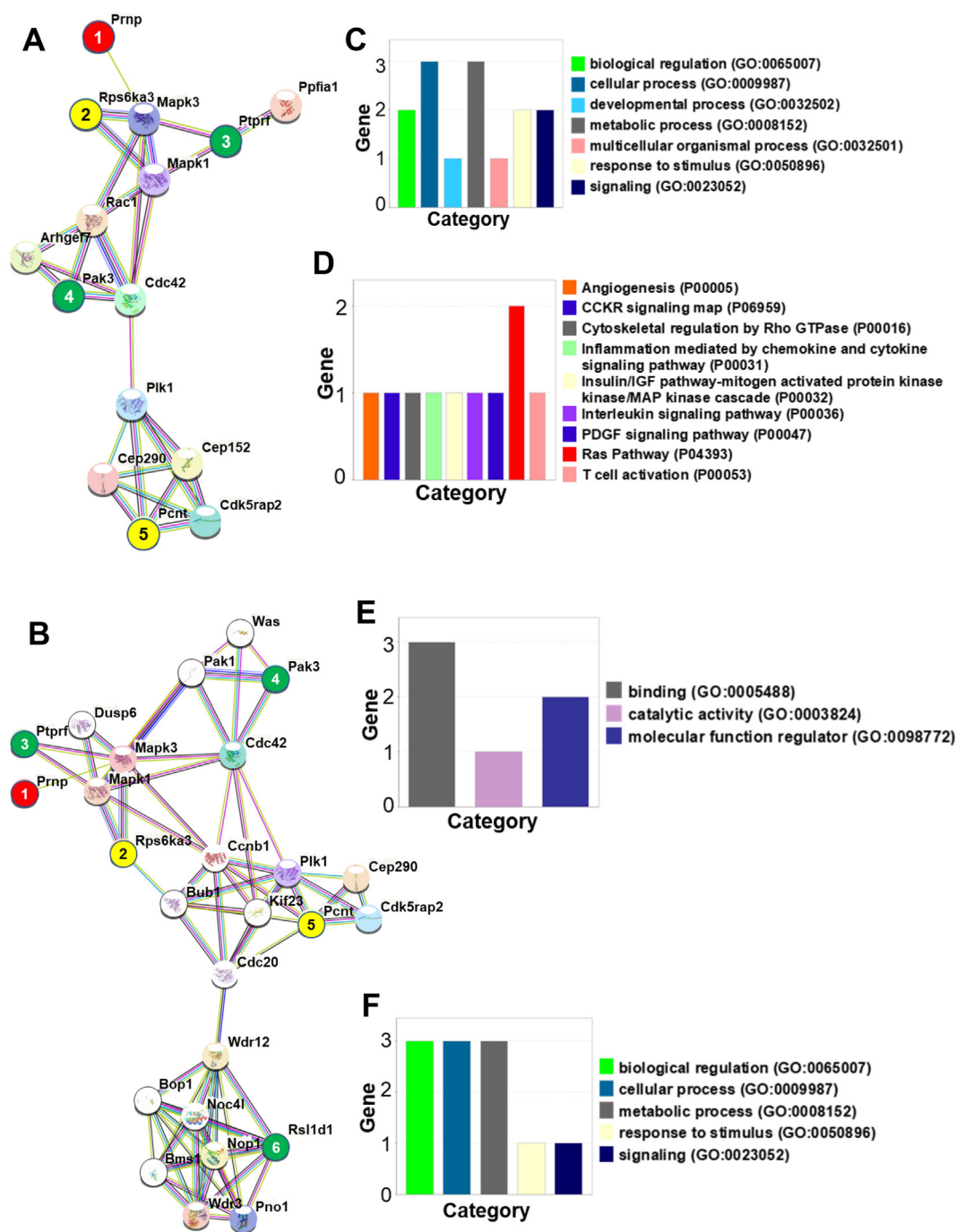


Figure 3. Protein-protein interaction and classification of the identified apoptotic genes following direct antibody treatment (DAT) to the neuroblastoma N2A cell line and primary neuronal cells. The protein-protein interaction analysis was performed using STRING v11.0 server and PANTHER server was used for the classification analysis. The *Mus musculus* database was used as the host organism for characterising the protein interactions and classification in both STRING v11.0 and PANTHER server. A) Interaction among the apoptotic proteins (numbered 2, 3, 4 & 5) with PrP^C (numbered 1) following direct antibody treatment. B) Interaction among the identified apoptotic proteins from cell line (numbered 2, 3, 4 & 5) and primary neuronal cells (numbered 6) with PrP^C (numbered 1) following direct antibody treatment. Classification of the C) biological processes; and D) signalling pathways of the identified apoptotic genes from neuroblastoma cell line compared to the untreated cells. Classification of the E) molecular function F) biological process of the identified apoptotic genes from primary neuronal cells compared to the 3F4 antibody treated cells.

Table 4. Properties of the identified apoptotic proteins following direct antibody treatment (DAT) and direct microglia treatment (DMT) of mouse primary neuronal cells. The properties were identified by Progenesis Software after the LC-MS analysis.

| | Sample | Accession | Gene ID | Protein Name | Peptides | Unique peptides | Confidence score | Anova (p) | Max fold change | Highest Mean | Lowest Mean |
|------------------------------------|----------------------------------|-----------|-----------|--|----------|-----------------|------------------|-----------|-----------------|--------------|-------------|
| Comparison with No Treatment (NoT) | Direct Antibody Treatment (DAT) | Q3TAJ5 | Rsl1d1 | ribosomal L1 domain containing 1 | 1 | 1 | 5.66 | 0.029092 | āz | DAT | CTL (NoT) |
| | Direct Microglia Treatment (DMT) | Q547V2 | Igf1 | Insulin-like growth factor 1 | 1 | 1 | 4.7 | 0.001422 | 68.3 | DMT | CTL (NoT) |
| | | Q9DBX1 | Rgcc | Regulator of cell cycle RGCC | 1 | 1 | 5.5 | 0.019531 | 16.7 | DMT | CTL (NoT) |
| | | D3YXU4 | Chil1 | Chitinase-like 1 (Fragment) | 1 | 1 | 5.39 | 0.019619 | 380 | CTL (NoT) | DMT |
| | | Q9D5K8 | Zfp819 | zinc finger protein 819 | 1 | 1 | 4.28 | 0.03142 | 14.6 | CTL (NoT) | DMT |
| Comparison with 3F4 | Direct Antibody Treatment (DAT) | A3KG38 | Ikbkg | kappa-B essential modulator (Fragment) | 1 | 1 | 4.62 | 0.000377 | 40.9 | DAT | 3F4 |
| | | Q5I2A0 | Serpina3g | Serine protease inhibitor A3G | 5 | 5 | 21.9 | 0.000556 | 10.9 | DAT | 3F4 |
| | | Q9D5K8 | Zfp819 | zinc finger protein 819 | 1 | 1 | 4.28 | 0.008202 | 21.9 | 3F4 | DAT |
| | Direct Microglia Treatment (DMT) | Q9D5K8 | Zfp819 | zinc finger protein 819 | 1 | 1 | 4.28 | 0.007086 | 11.1 | 3F4 | DMT |
| | | Q5NCK8 | Mapk9 | Mitogen-activated protein kinase | 1 | 1 | 6.09 | 0.039174 | 38.5 | DMT | 3F4 |

assess and analyse extensive genome-wide experimental data (Mi et al., 2019). In addition, the gene enrichment analysis was conducted on the identified final dataset of DAT, DMT and IMT using FunRich software v 3.1.3 (Pathan et al., 2017). FunRich is a stand-alone software tool used mainly for functional enrichment and interaction network analysis of genes and proteins (Pathan et al., 2015, 2017).

2.8. Statistical analyses

Statistical analyses were assessed by Student's t-test, Chi-Squared test or analysis of variance (ANOVA) test. The results were considered significant at $p < 0.05$.

3. Results

3.1. Treatment of neuroblastoma N2a cell lines with Anti-PrP antibodies leads to apoptosis

The overall workflow for the identification of apoptotic proteins and confirmation of apoptosis is shown in Figure 2. Treatment of N2a cells

with anti-PrP antibodies ICSM18, ICSM35, POM1 or SAF70 led to the identification of 27 proteins after liquid-chromatography mass spectrometry (LC-MS) analysis when compared with N2a cells treated only with tissue culture medium and no addition of antibodies. Differentially expressed proteins ($p < 0.05$) were considered with a maximum fold change ≥ 10 and at least 2 identified unique peptides and a confidence score ≥ 40 (Table 2 and Table S1).

After functional analysis of the 27 identified proteins using DAVID bioinformatics resources (Huang et al., 2009; Jiao et al., 2012), we found 4 proteins associated with the apoptotic process, including Receptor-type tyrosine-protein phosphatase F (PTPRF), Ribosomal Protein S6 Kinase A3 protein (RPS6KA3), p21-activated Kinase 3 (PAK3), and Pericentrin protein (PCNT) (Table 2). The functional annotation showed that RPS6KA3 is associated with negative regulation of cysteine-type endopeptidase activity involved in apoptotic process (Anjum et al., 2005; Carriere et al., 2008) whereas both PTPRF and PAK3 are involved in positive regulation of apoptosis (Bera et al., 2014; McPhie et al., 2003; Stewart et al., 2017). However, PCNT protein which displayed the highest mean in the untreated N2a cells, is involved in the negative regulation of apoptotic process (Kim et al., 2019; Zimmerman et al.,

Table 5. Identification of antibody-specific apoptotic proteins following direct antibody treatment (DAT) and direct microglia treatment (DMT) of mouse primary neuronal cells. (√) Upregulated and (-) Downregulated.

| | Comparison with No Treatment (NoT) | | | | | |
|----------------------------------|------------------------------------|-----------|--------|-----------|--------|-----------|
| | Accession ID | Gene ID | ICSM18 | CTL (NoT) | ICSM35 | CTL (NoT) |
| Direct Antibody Treatment (DAT) | Q3TAJ5 | Rsl1d1 | √ | - | √ | - |
| Direct Microglia Treatment (DMT) | Q547V2 | Igf1 | √ | - | √ | - |
| | Q9DBX1 | Rgcc | √ | - | √ | - |
| | D3YXU4 | Chil1 | - | √ | - | √ |
| | Q9D5K8 | Zfp819 | - | √ | - | √ |
| | | | | | | |
| | Comparison with 3F4 | | | | | |
| | Accession ID | Gene ID | ICSM18 | CTL (3F4) | ICSM35 | CTL (3F4) |
| Direct Antibody Treatment (DAT) | A3KG38 | Ikbkg | √ | - | √ | - |
| | Q5I2A0 | Serpina3g | √ | - | √ | - |
| | Q9D5K8 | Zfp819 | - | √ | - | √ |
| Direct Microglia Treatment (DMT) | Q5NCK8 | Zfp819 | √ | - | √ | - |
| | Q9D5K8 | Mapk9 | - | √ | - | √ |

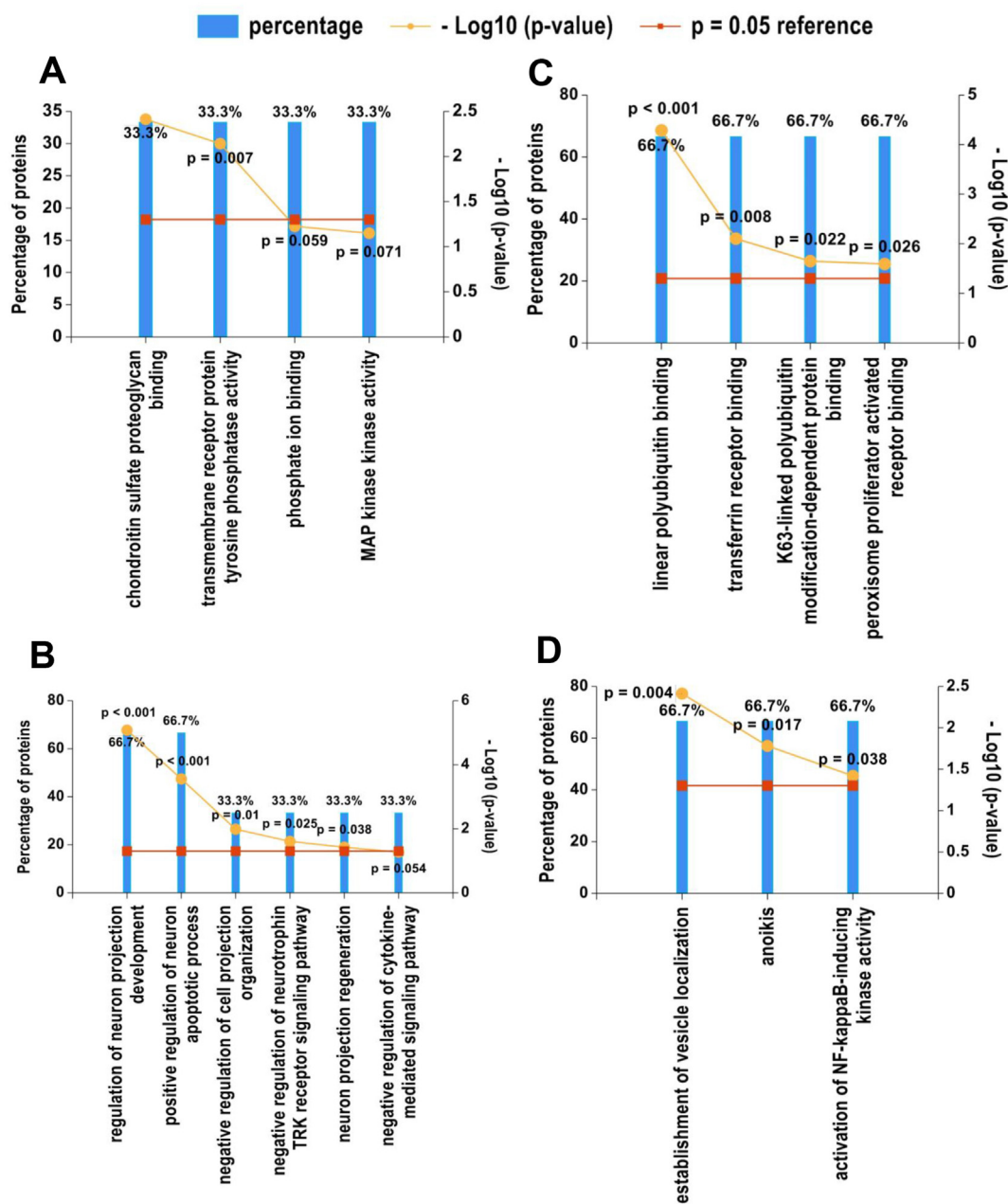


Figure 4. Gene enrichment analysis of the identified apoptotic genes following direct anti-PrP antibody treatment (DAT) to the neuroblastoma cell line and primary neuronal cells. Classification of the A) molecular functions; and B) biological processes of the identified 4 apoptotic genes following direct anti-PrP antibody treatment (DAT) to the N2A cells compared to the untreated N2A cells. Classification of the C) molecular functions; D) biological processes of the identified 2 apoptotic genes following direct anti-PrP antibody treatment (DAT) to the primary neuronal cells compared to the 3F4 antibody treated cells. Functional gene enrichment analysis was performed using FunRich software (v3.1.3). The p -value in the plot is the Bonferroni corrected p -value and the reference p -value is $p = 0.05$.

2004) (Table S2). Analysis of individual anti-PrP antibody treatment effect on N2a cells revealed that RPS6KA3 and PCNT were present after direct ICSM18 treatment (Table 3). However, direct treatment with ICSM35, POM1 and SAF70 was not associated with apoptosis proteins.

It should be noted that for PCNT, the highest mean was associated with untreated N2a cells and might reflect its downregulation as a result of antibody treatment leading to apoptosis following upregulation of PTPRF and PAK3 via MAPK3 stimulation/upregulation (Table 2 & Figure 3A). Protein-protein interaction (STRING, Version 11.0) analysis of PTPRF, PAK3, RPS6KA3 were shown to be part of the same protein network as PrP^C whereas the downregulated PCNT was not identified as a PrP^C interactor (Figure 3A). Interestingly, PrP^C was shown to interact directly with MAPK3 which in turn directly interacts with RPS6KA3 and

PTPRF and indirectly with PAK3 via RAC1 protein (Figure 3A). However, PrP^C did not interact with PCNT directly but required stimulation of at least another 3 proteins (Figure 3A).

3.2. Treatment of primary neuronal cells with Anti-PrP antibodies leads to apoptosis

In order to verify the biological relevance of the anti-PrP antibody neurotoxic effects, we treated mouse primary neuronal cells (Haigh et al., 2011) with 1 μg ICSM18 or ICSM35 anti-PrP antibodies. This led to the identification of 32 proteins after the LC-MS analysis when compared with untreated cells (Table S3). In order to confirm the specificity of the apoptotic effect of these anti-PrP antibodies, we treated the primary

Table 6. Properties of the identified apoptotic proteins following direct microglia treatment (DMT) of neuroblastoma cell line. The properties were identified by Progenesis Software after the LC-MS analysis.

| Gene ID | Accession | Protein Name | Peptides | Unique peptides | Confidence score | Anova (p) | q Value | Max fold change | Highest Mean | Lowest Mean |
|----------|------------|---|----------|-----------------|------------------|-----------|----------|-----------------|-------------------------|-------------------------|
| APBB1 | A0A0R4J2C1 | Amyloid-beta A4 precursor protein-binding family B member 1 | 9 | 5 | 52.1 | 0.002787 | 0.002517 | 11.5 | Direct Microglia Effect | Control |
| ANK2 | S4R2T7 | Ankyrin-2 (Fragment) | 11 | 6 | 75.2 | 3.53E-11 | 4.03E-10 | 12.2 | Direct Microglia Effect | Control |
| CASP8AP2 | Q9WUF3 | CASP8-associated protein 2 | 28 | 10 | 171 | 4.59E-07 | 1.34E-06 | 11.9 | Direct Microglia Effect | Control |
| CUL1 | Q05DR6 | Cul1 protein (Fragment) | 9 | 3 | 46.7 | 1.06E-13 | 2.76E-12 | 11.4 | Direct Microglia Effect | Control |
| CUL7 | A9C491 | Cullin 7 | 12 | 4 | 56.7 | 5E-08 | 1.92E-07 | 1210 | Control | Direct Microglia Effect |
| DOCK1 | Q8BUR4 | Dedicator of cytokinesis protein 1 | 11 | 5 | 60.1 | 2.23E-08 | 9.74E-08 | 13.8 | Control | Direct Microglia Effect |
| FNDC1 | E9Q043 | Fibronectin type III domain-containing 1 | 13 | 7 | 67.9 | 1.66E-09 | 1.06E-08 | 16.4 | Control | Direct Microglia Effect |
| INTS1 | K3W4P2 | Integrator complex subunit 1 | 43 | 8 | 228 | 9.03E-09 | 4.55E-08 | 41.3 | Direct Microglia Effect | Control |
| LGMN | A2RTI3 | Legumain | 8 | 2 | 51.3 | 3.27E-07 | 1.01E-06 | 443 | Direct Microglia Effect | Control |
| MT1 | P02802 | Metallothionein-1 | 7 | 3 | 66.1 | 0.004504 | 0.003806 | 12.8 | Control | Direct Microglia Effect |
| PDE1A | Q61481 | Calcium/calmodulin-dependent 3',5'-cyclic nucleotide phosphodiesterase 1A | 10 | 2 | 60.6 | 4.35E-14 | 1.26E-12 | 24.7 | Control | Direct Microglia Effect |
| PHB2 | O35129 | Prohibitin-2 | 18 | 3 | 160 | 1.45E-09 | 9.48E-09 | 22.8 | Control | Direct Microglia Effect |
| PTPRC | P06800 | Receptor-type tyrosine-protein phosphatase C | 6 | 2 | 41.1 | 6.11E-07 | 1.72E-06 | 12.5 | Direct Microglia Effect | Control |
| RAG1 | Q78NA6 | V(D)J recombination-activating protein 1 | 16 | 5 | 95.2 | 2.91E-13 | 6.9E-12 | 13.5 | Direct Microglia Effect | Control |
| RPS3 | Q3UK56 | KH type-2 domain-containing protein | 21 | 2 | 201 | 1.04E-08 | 5.05E-08 | 10.5 | Direct Microglia Effect | Control |
| SEMA6A | D3YWM8 | Semaphorin-6A | 10 | 3 | 56.5 | 4.86E-07 | 1.41E-06 | 40.8 | Direct Microglia Effect | Control |
| TLR3 | Q3TM31 | TIR domain-containing protein | 9 | 2 | 43.2 | 0.043612 | 0.026424 | 14.8 | Direct Microglia Effect | Control |

neuronal cells with the 3F4 antibody, previously shown to react with hamster but not mouse PrP (Kasczak et al., 1987). Here, 22 proteins were identified following LC-MS analysis when compared to treatment with 1 µg of 3F4 antibody (Table S4). After functional analysis of the 32 (vs. no treatment) and 22 (vs. 3F4) proteins using DAVID bioinformatics resources, we found 1 (Ribosomal L1, 1RSL1D1) and 3 (Inhibitor of kappaB kinase gamma, IKBKG - SERPINA3G, Serine peptidase inhibitor, clade A, member 3G - zinc finger protein 819, ZFP819) apoptotic related proteins, respectively (Table S2 and Table S5). 1RSL1D1 has previously been shown to regulate apoptosis (Li et al., 2012; Ma et al., 2015). IKBKG was found to be associated with intrinsic apoptotic signalling pathway (Frelin

et al., 2008) while SERPINA3G was shown to be involved in the apoptotic process (Liu et al., 2003). However, ZFP819 which displayed highest mean in the 3F4 treatment was reported to be associated with positive regulation of the apoptotic process (Jin et al., 2017) (Table 4 and Table S2).

Analysis of individual anti-PrP antibody treatment effect on MPN cells revealed that RSL1D1, IKBKG, SERPINA3G and ZFP819 were present after ICSM18 and ICSM35 treatments (Table 5). Since the identified apoptotic related proteins were found to be different between antibody treated N2a cells and primary neuronal cells, we performed protein-protein interaction analysis through STRING server (version 11.0) to

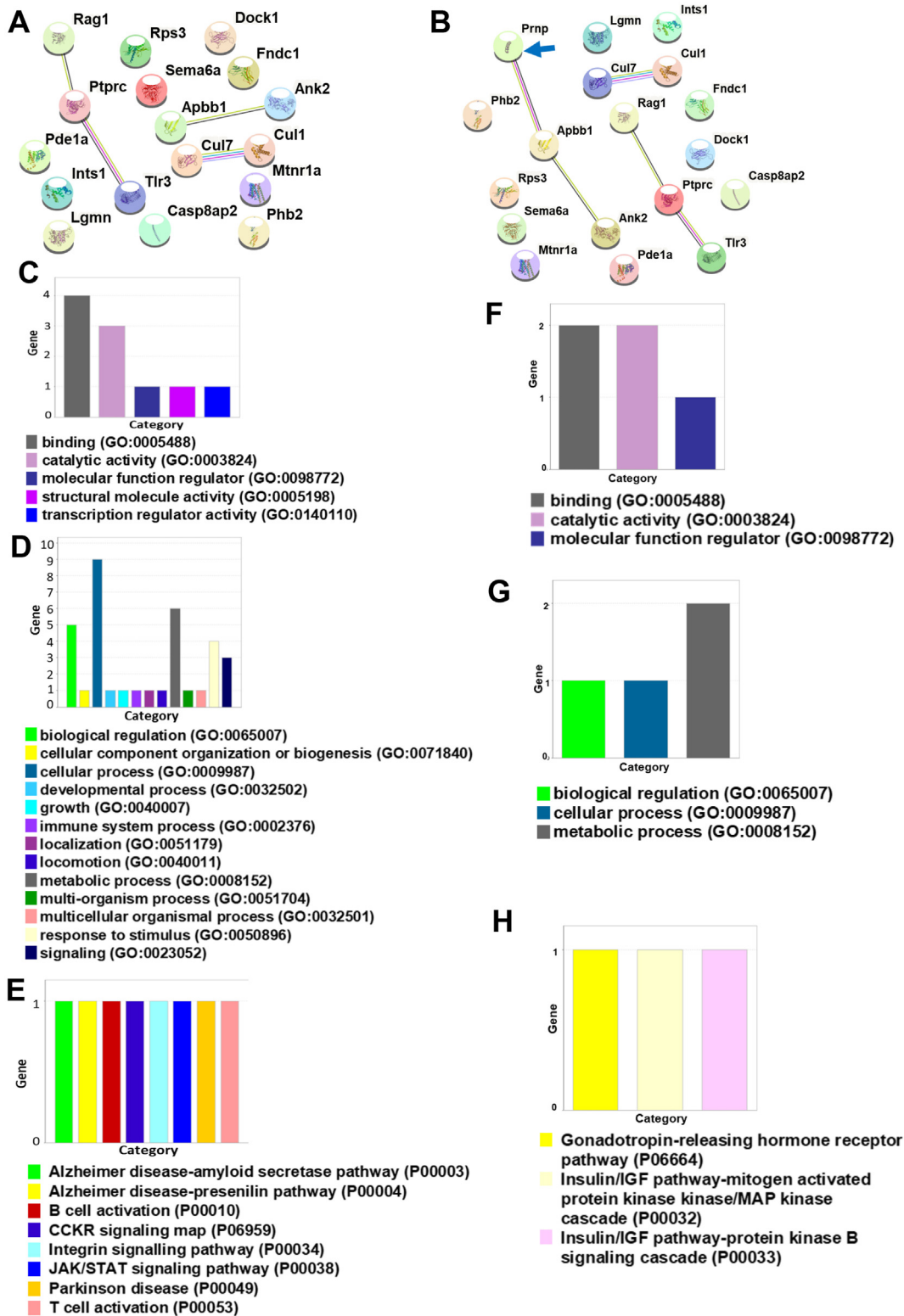


Figure 5. Protein-protein interaction and classification analysis among the identified apoptotic genes following direct microglial treatment (DMT) with anti-PrP antibodies. The protein-protein interaction analysis was performed using STRING v11.0 server and PANTHER server was used for the classification analysis. The *Mus musculus* database was used as the host organism for characterising the protein interactions and classification in both STRING v11.0 and PANTHER server. A) displays interactions among the 17 identified apoptotic genes and B) displays interactions between the *Prnp* gene and the 17 identified apoptotic genes following direct microglial treatment (DMT) to the cell line. Classification of the C) molecular function; D) biological processes; and E) signalling pathways of the identified apoptotic genes from neuroblastoma cell line compared to the untreated cells. Classification of the F) molecular function; G) biological process; and H) signalling pathways of the identified apoptotic genes from primary neuronal cells compared to the untreated cells.

Table 7. Identification of antibody-specific apoptotic proteins following direct microglia treatment (DMT) of neuroblastoma cell lines.

| Accession ID | Gene ID | Effect of Different Anti-PrP Antibodies | | | | | | | | | | | | | |
|--------------|----------|---|-----|--------|-----|----------------|-----|------|-----|------|-----|----------------|-----|-------|-----|
| | | ICSM Antibodies | | | | POM Antibodies | | | | | | SAF Antibodies | | | |
| | | ICSM18 | CTL | ICSM35 | CTL | POM1 | CTL | POM2 | CTL | POM3 | CTL | SAF32 | CTL | SAF70 | CTL |
| A0A0R4J2C1 | Apbb1 | - | - | - | - | √ | - | √ | - | √ | - | - | - | - | - |
| S4R2T7 | Ank2 | √ | - | - | - | - | - | √ | - | - | - | √ | - | √ | - |
| Q9WUF3 | Casp8ap2 | - | - | √ | - | - | - | √ | - | - | - | √ | - | - | - |
| Q05DR6 | Cul1 | √ | - | √ | - | - | - | √ | - | √ | - | - | - | √ | - |
| A9C491 | Cul7 | - | √ | - | √ | - | √ | - | √ | - | √ | - | √ | - | √ |
| Q8BUR4 | Dock1 | - | √ | - | - | - | - | - | √ | - | √ | - | √ | - | √ |
| E9Q043 | Fndc1 | - | √ | - | √ | - | √ | - | √ | - | √ | - | √ | - | √ |
| K3W4P2 | Ints1 | √ | - | √ | - | - | - | √ | - | √ | - | √ | - | √ | - |
| A2RTI3 | Lgmn | √ | - | √ | - | - | - | √ | - | √ | - | √ | - | √ | - |
| P02802 | Mt1 | - | √ | - | √ | - | - | - | √ | - | √ | - | √ | - | √ |
| Q61481 | Pde1a | - | √ | - | √ | - | √ | - | √ | - | √ | - | √ | - | √ |
| O35129 | Phb2 | - | √ | - | √ | - | √ | - | √ | - | √ | - | √ | - | √ |
| P06800 | Ptprc | √ | - | √ | - | - | - | - | - | - | - | √ | - | √ | - |
| Q78NA6 | Rag1 | √ | - | √ | - | √ | - | √ | - | - | - | √ | - | √ | - |
| Q3UK56 | Rps3 | √ | - | - | - | - | - | √ | - | - | - | √ | - | - | - |
| D3YWM8 | Sema6a | √ | - | √ | - | - | - | √ | - | √ | - | √ | - | √ | - |
| Q3TM31 | Tlr3 | - | - | - | - | √ | - | √ | - | - | - | - | - | - | - |

(√) Upregulated and (-) Downregulated.

verify whether these proteins belong to the same interactome. We found that RSL1D1 interacts with PCNT, PTPRF, RPS6KA3 and PAK3 via Wdr12 (Figure 3B) while IKBKG and SERPINA3G belonged to the same protein 'hub'.

3.3. Gene ontology (GO) analysis of apoptosis related proteins associated with direct antibody treatment

Using PANTHER classification system (v.14.0) (Mi et al., 2019), a gene classification server and FunRich (Functional Enrichment analysis tool – Version 3.1.3) (Pathan et al., 2015) protein Gene enrichment software (reference list “rodent database”), we performed Gene Ontology (GO) analysis for molecular function, biological process, and the signalling pathway.

PANTHER identified RPS6KA3, PTPRF, PAK3 apoptotic related genes involved in molecular functions, biological processes and signalling pathways. The molecular function of RPS6KA3, PTPRF, PAK3 genes were found to be associated with catalytic activity. The biological process of both PTPRF and PAK3 was found to be associated with metabolic process, biogenesis and cellular process. Moreover, PAK3 was found to be involved in signalling, response to stimulus, multicellular organismal process, developmental process, and biological regulation whereas PTPRF was found to be associated with biological adhesion (Figure 3C). Signalling pathway analysis identified both RPS6KA3 and PAK3 association with the Ras Pathway (Figure 3D). The signalling pathway analysis of the PAK3 was found to be associated with angiogenesis, cytoskeletal regulation by Rho GTPase, inflammation mediated by chemokine and cytokine signalling pathway, and T cell activation (Figure 3D). On the other hand, RPS6KA3 was found to be involved in CCKR signalling map, IGF pathway-mitogen activated protein kinase kinase/MAP kinase cascade, interleukin signalling pathway, and PDGF signalling pathway (Figure 3D).

Further gene ontology analysis of the apoptotic related proteins (IKBKG, SERPINA3G, and ZFP819) identified following treatment of primary neuronal cells revealed molecular function and biological processes (Figure 3E and F). The molecular function of SERPINA3G was found to be associated with binding, catalytic activity, and molecular function regulator whereas ZFP819 was found to be involved in binding and molecular function regulator and IKBKG is involved in binding activity (Figure 3E). The biological process analysis of the IKBKG was found

to be associated with biological regulation, cellular process, metabolic process, response to stimulus, and signalling pathway. On the other hand, both SERPINA3G and ZFP819 were found to be involved in biological regulation and metabolic process (Figure 3F).

FunRich analysis revealed two significant molecular functions, including chondroitin sulfate proteoglycan binding (PTPRF; $p = 0.004$), and transmembrane receptor protein tyrosine phosphatase activity (PTPRF; $p = 0.007$) (Figure 4A). FunRich also identified several biological processes, including positive regulation of neuron apoptosis process (PTPRF, PAK3; $p < 0.001$), regulation of neuron projection development (PTPRF, PAK3; $p < 0.001$), negative regulation of cell projection organization (PTPRF; $p = 0.01$), negative regulation of neurotrophin TRK receptor signaling pathway (PTPRF; $p = 0.025$), and neuron projection regeneration (PTPRF; $p = 0.038$) (Figure 4B).

Further FunRich analysis of the IKBKG, SERPINA3G, and ZFP819 revealed several molecular functions, including peroxisome proliferator activated receptor binding (IKBKG; $p = 0.026$), K63-linked polyubiquitin modification-dependent protein binding (IKBKG; $p = 0.022$), transferrin receptor binding (IKBKG; $p = 0.007$), linear polyubiquitin binding (IKBKG; $p < 0.001$) (Figure 4C). FunRich also identified several biological processes including activation of NF-kappaB-inducing kinase activity (IKBKG; $p = 0.038$), negative regulation of endoplasmic reticulum stress-induced intrinsic apoptotic signalling pathway (IKBKG; $p = 0.077$), anoikis (IKBKG; $p = 0.017$), and establishment of vesicle localization (IKBKG; $p = 0.003$) (Figure 4D).

3.4. Co-culture of Anti-PrP antibody treated-microglia N11 with N2a cell lines leads to apoptosis of N2a cells

Co-culture of N2a cells with N11 cells treated with anti-PrP antibodies ICSM18, ICSM35, POM1, POM2, POM3, SAF32 or SAF70 led to the identification of 113 proteins after LC-MS analysis when compared with co-culture of N2a with untreated-N11 cells. Differentially expressed proteins ($p < 0.05$) were considered with a maximum fold change ≥ 10 and at least 2 identified unique peptides and a confidence score ≥ 40 (Table S6). The functional analysis of the identified 113 proteins showed that 17 proteins are associated with apoptosis (Table 6 and Table S2).

Among the identified apoptotic proteins Amyloid-beta A4 precursor protein-binding family B member 1 (APBB1), Fibronectin type III domain-containing 1 (FNDC1), KH type-2 domain-containing protein

(RPS3) and TIR domain-containing protein (TLR3) are associated with positive regulation of the apoptotic process (Jang et al., 2004, 2012; Salaun et al., 2006; Sato et al., 2009) whereas Integrator complex subunit 1 (INTS1), Legumain (LGMN), Metallothionein-1 (MT1), Prohibitin-2 (PHB2), and V(D)J recombination-activating protein 1 (RAG1) proteins are involved in the negative regulation of the apoptotic process (Andrade et al., 2011; Hata and Nakayama, 2007; Novoa et al., 2019; Shimoda et al., 2003; Sun et al., 2018; Yang et al., 2018). In addition, CASP8-associated protein 2 (CASP8AP2), Receptor-type tyrosine-protein phosphatase C (PTPRC) and TIR domain-containing protein (TLR3) proteins identified in the dataset play a role in the extrinsic apoptotic signalling pathway (Hanaoka et al., 1995; Salaun et al., 2006; Sun et al., 2011; Wang and Lenardo, 2000) whereas RPS3 protein is involved in intrinsic apoptotic signalling pathway (Jang et al., 2004, 2012) (Table S2). Among the identified 17 apoptotic proteins, 11 (APBB1, ANK2, CASP8AP2, CUL1, INTS1, LGMN, PTPRC, RAG1, RPS3, SEMA6A, TLR3) showed the highest mean for DMT when compared with N2a cultured with untreated-N11 cells (Table 6). On the contrary, the remaining 6 proteins (CUL7, DOCK1, FNDC1, MT1, PDE1A, PHB2) exhibited highest mean values for N2a cultured with untreated-N11 cells indicating that downregulation of these proteins following anti-PrP antibody treatment might be involved in the apoptosis process (Table 6).

Protein-protein interaction (STRING, Version 11.0) analysis of the identified 7 out of 11 apoptotic proteins with highest mean following co-culture of N2a cells with antibody-treated N11 (APBB1, ANK2, CUL1, INTS1, PTPRC, RAG1, TLR3) were shown to be part of the same protein network as PrP^C (Figure 5A and B). Interestingly, protein-protein

interaction analysis of the 6 identified apoptotic related proteins with lowest mean (CUL7, DOCK1, FNDC1, MT1, PDE1A, PHB2) following co-culture of N2a cells compared with untreated N11 were not part of PrP^C network, suggesting that their downregulation is probably caused by negative feedback interaction associated with PrP^C. For instance, CUL1 which interacts directly with PrP^C, also interacts with CUL7 (Table 6). Interestingly and with the exception of SAF32, and POM1 all other antibodies tested, including ICSM18, ICSM35, POM2, POM3 and SAF70 displayed highest mean of CUL1 and lowest mean of CUL7 confirming cross-feedback between these 2 proteins (Table 6 and Table 7). Table 7 provides details of highest versus lowest mean protein expression caused by individual antibody treatment. This shows that ICSM18 and SAF32 share 47.05% apoptotic proteins (7 proteins: ANK2, INTS1, LGMN, PTPRC, RAG1, RPS3, SEMA6A) and ICSM35 and SAF70 share 41.17% apoptotic proteins (6 proteins: CUL1, INTS1, LGMN, PTPRC, RAG1, SEMA6A). POM2 showed highest effect on expression of apoptotic proteins with 58.82% (10 proteins: APBB1, ANK2, CASP8AP2, CUL1, INTS1, LGMN, PTPRC, RAG1, SEMA6A, TLR3), and the lowest effect was observed for the POM1 treatment (17.64% with 3 proteins: APBB1, RAG1, and TLR3) and POM3 (29.41% with 5 proteins: APBB1, CUL1, INTS1, LGMN, SEMA6A).

3.5. Co-culture of Anti-PrP antibody treated-microglia N11 with primary neuronal cells leads to apoptosis of neuronal cells

Prior to co-culturing of anti-PrP antibody treated N11 microglia with the primary neuronal cells, we performed immunofluorescence analysis to confirm the mouse neuronal stem cells were differentiated into

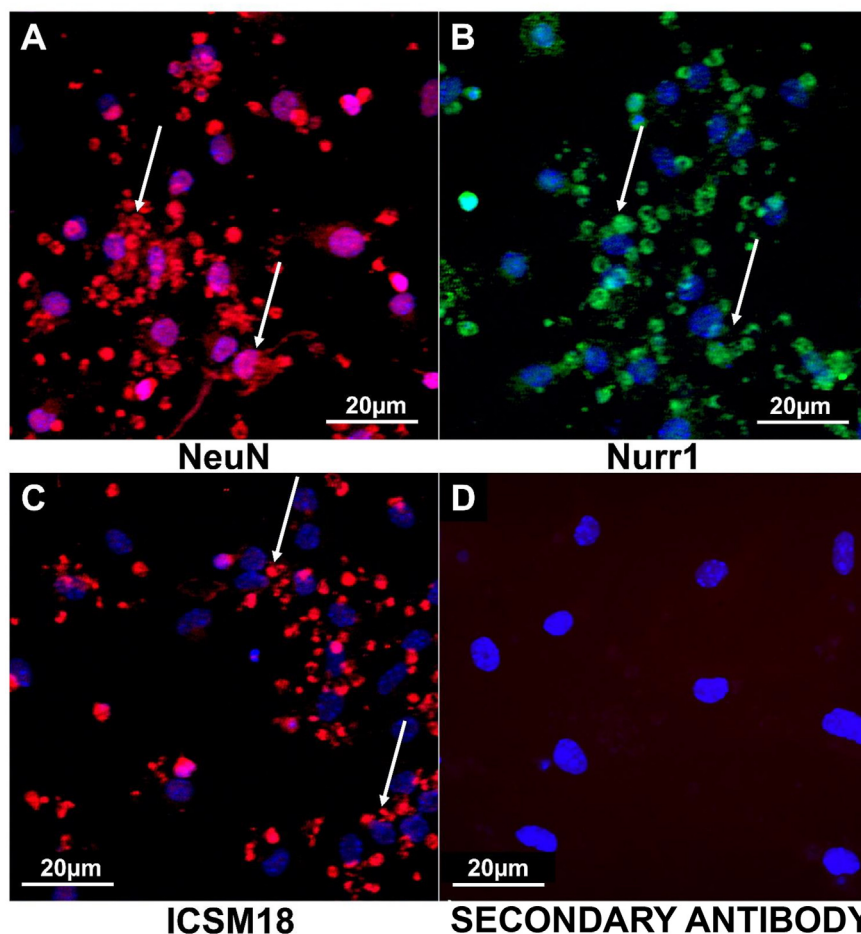


Figure 6. Immunofluorescence analysis of the fully differentiated primary neuronal cells. Here, NeuN and Nurr1 were used for the identification of neuronal marker and ICSM18 was used for the detection of PrP^C expression.

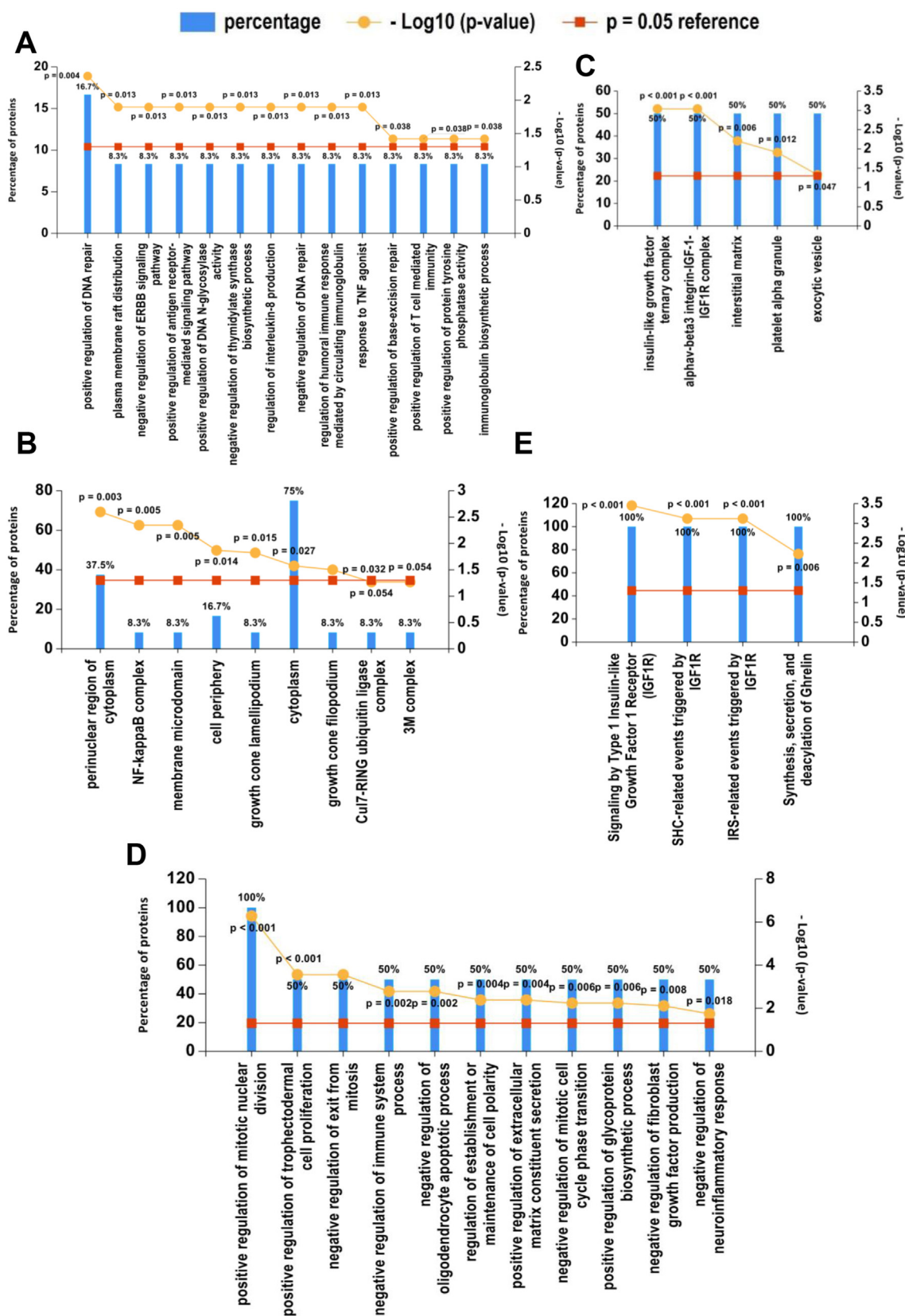


Figure 7. Gene enrichment analysis of the identified apoptotic genes following direct microglia treatment (DMT) to the neuroblastoma cell line and primary neuronal cells. Classification of the A) biological processes; and B) cellular components of the identified 17 apoptotic genes following direct microglia treatment (DMT) to the N2A cells compared to the untreated cells. Classification of the C) cellular components; D) biological processes; and E) reactome pathway of the identified 4 apoptotic genes following direct microglia treatment (DMT) to the primary neuronal cells compared to the untreated cells. Functional gene enrichment analysis was performed using FunRich software (v3.1.3). The *p*-value in the plot is the Bonferroni corrected *p*-value and the reference *p*-value is *p* = 0.05.

neurons (MPN) expressing the cellular prion protein using Neuronal Nuclei (NeuN), Nur-related factor (Nurr1) and ICSM18 antibodies. The positive staining of both NeuN and Nurr1 and PrP^C indicated that the mouse neuronal stem cells were fully differentiated into neurons (MPN) (Figure 6).

Co-culture of MPN cells with N11 treated with 1 µg of ICSM18 or ICSM35 led to the identification of 25 proteins after LC-MS analysis when compared with co-culture of MPN cells with untreated N11 cells (Table S7) while 8 proteins were identified when compared to treatment with 3F4 antibody (Table S8). The functional annotation of the identified 25 proteins showed that 4 proteins are associated with apoptosis whereas the analysis of 8 proteins revealed 2 apoptosis related proteins (Table 4 and Table S2). Among the identified apoptosis related proteins, Mitogen-activated protein kinase 9 (MAPK9), Zinc finger protein 819 (ZFP819) and Regulator of cell cycle (RGCC) are associated with positive regulation of the apoptotic process (Table S2). However, Insulin-like growth factor 1 (IGF1) is involved in negative regulation of apoptosis and negative regulation of extrinsic apoptotic signalling pathway whereas chitinase-like 1 (CHIL1) was found to be involved in the apoptotic process (Table S2). Among the identified 4 apoptosis related proteins, IGF1 and RGCC showed the highest mean for DMT when compared with MPN cells cultured with untreated N11 cells (Table 4). On the contrary, CHIL1 and ZFP819 exhibited the highest mean for the MPN cells cultured with untreated N11 cells indicating their downregulation following anti-PrP antibody (ICSM18 and ICSM35) treatment (Table 4). ZFP819 was also found to be downregulated when compared with 3F4 antibody treatment (Table 4).

Protein-protein interaction (STRING, Version 11.0) analysis of the identified 4 apoptotic proteins (IGF1, RGCC, CHIL1, ZFP819) following co-culture of the MPN cells with antibody treated N11 cells were shown to be part of the same protein network as PrP^C (Figure S1). The interaction analysis among the identified 4 apoptotic proteins following co-culture of the MPN cells with antibody treated N11 cells and the identified 17 apoptotic proteins following co-culture of the N2a cells with antibody treated N11 cells were found to be part of the same protein network as PrP^C except for CHIL1, MT1, CASP8AP2, FNDC1 and PDE1A (Figure S2). Interestingly, these non-interacting proteins (except CASP8AP2) were found to be downregulated indicating their contribution to the apoptotic process following anti-PrP antibody treatment (Table 4 and Table 6).

The 2 apoptosis related proteins identified following co-culture of the MPN cells with 3F4 antibody treated N11 cells and the 17 apoptotic proteins identified following co-culture of the N2a cells with antibody treated N11 cells were found to be part of the same protein network as PrP^C except the proteins MT1, CASP8AP2, FNDC1, and PDE1A (Figure S3).

3.6. Gene ontology analysis of apoptosis related proteins associated with direct microglia treatment

PANTHER analysis identified the DMT related apoptotic proteins as being involved in different molecular functions, biological processes and pathways (Figure 5). The molecular function was categorized into 5 different groups as detailed in Figure 5C where it was observed that ANK2, TLR3, APBB1, RPS3, CUL1, SEMA6A were shown to be involved in binding activity and PDE1A, LGMN, RPS3, PTPRC are associated with catalytic activity. On the other hand, SEMA6A and CASP8AP2 are involved in molecular function regulator and transcription regulator activity, respectively (Table S9). Cellular components were found to be categorized into 10 groups with PANTHER analysis including cell, extracellular region, membrane, membrane-enclosed lumen, organelle, and protein-containing complex (Table S9). SEMA6A was shown to be located in the membrane and extracellular region of the cell. On the other hand, RPS3, INTS1, CUL1 were found to be involved in cell and protein-

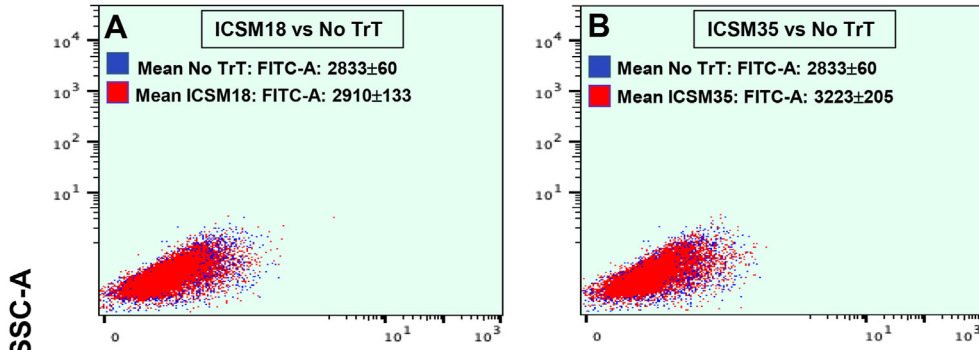
containing complex (Table S9). However, TLR3 was found to be located in the cell membrane and CASP8AP2 is associated with 3 different locations, including, membrane-enclosed lumen and organelle (Table S9). The biological process analysis (Figure 5D) showed that SEMA6A is associated with most functions except immune system process, metabolic process, and multi-organism process, while CASP8AP2 was shown to be involved in biological regulation, cellular process, metabolic process, response to stimulus and signaling pathway (Table S9). The signaling pathway is divided into 8 groups (Figure 5E) in which PTPRC is found to be associated with B cell activation, JAK/STAT signaling pathway, and T cell activation while DOCK1 is associated with the Integrin signaling pathway (Table S9).

PANTHER analysis of the identified apoptotic related proteins (IGF1, RGCC, CHIL1, ZFP819) observed in the primary neuronal cells revealed their involvement in molecular function, biological process and pathways. The molecular functions were found to be categorized into 3 groups, including binding (ZFP819, CHIL1), catalytic activity (CHIL1), and molecular function regulator (ZFP819) (Figure 5F). The biological process analysis showed that ZFP819 is involved in biological regulation and cellular process whereas both ZFP819 and CHIL1 are involved in metabolic process (Figure 5G). In pathway analysis, only IGF1 was found to be associated with gonadotropin-releasing hormone receptor pathway, insulin/IGF pathway-mitogen activated protein kinase kinase/MAP kinase cascade, and insulin/IGF pathway-protein kinase B signalling cascade (Figure 5H). For the 2 apoptotic proteins (MAPK9 and ZFP819), the molecular function was categorized into 3 groups where ZFP819 was associated with both binding and molecular function regulator and MAPK9 was involved in catalytic activity (data not shown).

FunRich analysis revealed a single significant molecular function, namely oxidized pyrimidine DNA binding ($p = 0.004$) (data not shown). Herein, FunRich analysis for the biological process, showed statistically significant biological process such as positive ($p = 0.004$) and negative ($p = 0.013$) regulation of DNA repair, positive regulation of DNA N-glycosylase activity, positive regulation of antigen receptor-mediated signalling pathway ($p = 0.013$), and negative regulation of thymidylate synthase biosynthetic process ($p = 0.013$) (Figure 7A). The functional enrichment analysis of the cellular components identified significant components such as perinuclear position of cytoplasm ($p = 0.003$), cytoplasm ($p = 0.026$), membrane micro domain ($p = 0.005$), NF-κB complex ($p = 0.005$), cell periphery ($p = 0.012$), growth cone lamellipodium ($p = 0.015$) and growth cone filopodium ($p = 0.031$) with statistically significant p value (Figure 7B).

FunRich analysis of the 4 apoptotic proteins (IGF1, RGCC, CHIL1, ZFP819) from primary neuronal cells when co-cultured with anti-PrP antibody treated N11 and compared with untreated N11 revealed the following: identified the important components for IGF1, including insulin-like growth factor ternary complex ($p = 0.002$), interstitial matrix ($p = 0.010$), platelet alpha granule ($p = 0.021$), and alphav-beta3 integrin-IGF-1-IGF1R complex ($p = 0.002$) (Figure 7C). The functional enrichment analysis of the biological process (Figure 7D) identified positive regulation of extracellular matrix constituent secretion (RGCC; $p = 0.007$), negative regulation of fibroblast growth factor production (RGCC; $p = 0.013$), negative regulation of oligodendrocyte apoptotic process (IGF1; $p = 0.003$), negative regulation of cholangiocyte apoptotic process (IGF1; $p = 0.007$), negative regulation of immune system process (IGF1; $p < 0.001$), negative regulation of neuroinflammatory response (IGF1; $p = 0.030$), positive regulation of trophectodermal cell proliferation (IGF1; $p < 0.001$), regulation of establishment or maintenance of cell polarity (IGF1; $p = 0.007$), negative regulation of exit from mitosis (RGCC; $p < 0.001$), negative regulation of mitotic cell cycle phase transition (RGCC; $p = 0.009$), positive regulation of mitotic nuclear division (RGCC and IGF1; $p < 0.001$), and positive regulation of glycoprotein biosynthetic process (IGF1; $p = 0.009$) (Figure 7D). Finally, FunRich analysis for the reactome pathway showed the significant pathways for

Direct Antibody Treatment (DAT) – Cell Lines



Direct Microglia Treatment (DMT) – Cell Lines

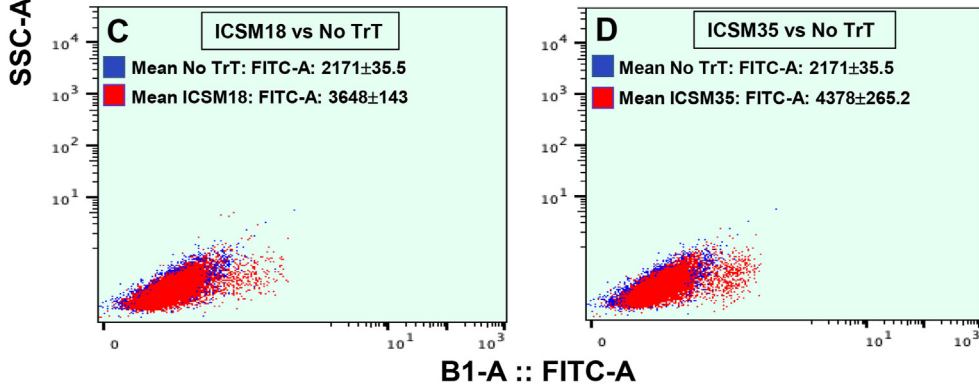
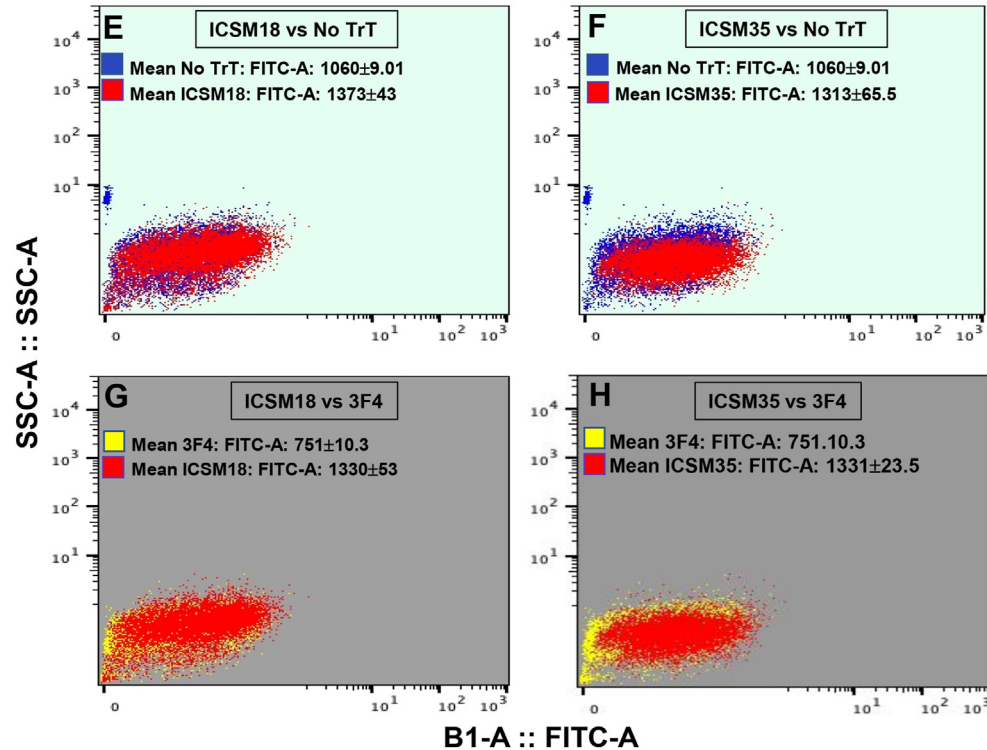


Figure 8. Flow cytometry analysis of live antibody-treated cells. A) Annexin V-FITC staining of direct ICSM18 antibody treated N2a cells in comparison with untreated N2a cells B) Annexin V-FITC staining of direct ICSM35 antibody treated N2a cells in comparison with untreated N2a cells C) Annexin V-FITC staining of direct ICSM18 antibody treated N11 cells co-cultured with N2a cells comparing with untreated cells (DMT) D) Annexin V-FITC staining in direct ICSM35 antibody treated N11 cells co-cultured with N2a cells (DMT) comparing with untreated cells E) Annexin V-FITC staining of direct ICSM18 antibody treated N11 cells co-cultured with primary neuronal cells in comparison with untreated cells F) Annexin V-FITC staining of direct ICSM35 antibody treated N11 cells co-cultured with primary neuronal cells in comparison with untreated cells G) Annexin V-FITC staining of direct ICSM18 antibody treated N11 cells co-cultured with primary neuronal cells in comparison with 3F4 treated cells H) Annexin V-FITC staining of direct ICSM35 antibody treated N11 cells co-cultured with primary neuronal cells (DMT) comparing with 3F4 treated cells.

Direct Microglia Treatment (DMT) – Mouse Primary Neurons



the IGF1 (Figure 7E), including synthesis, secretion, and deacylation of ghrelin ($p = 0.006$), signalling by Type 1 insulin-like growth Factor 1 receptor (IGF1R) ($p < 0.001$), SHC-related events triggered by IGF1R ($p < 0.001$), IRS-related events triggered by IGF1R ($p < 0.001$) (Figure 7E).

FunRich analysis identified the molecular function, biological process and reactome pathways for the identified 2 apoptotic proteins (MAPK9 and ZFP819) from primary neuronal cells when co-cultured with anti-PrP antibody treated N11 compared with 3F4 antibody treated N11. The FunRich analysis of the molecular function identified the significant molecular function for the MAPK9, including cysteine-type endopeptidase activator activity involved in apoptotic process ($p = 0.008$), mitogen-activated protein kinase kinase binding ($p = 0.042$), JUN kinase activity ($p = 0.001$), and MAP kinase activity ($p = 0.018$) (Figure S4A). The functional enrichment analysis of the biological process identified several biological processes including positive regulation of macrophage derived foam cell differentiation (MAPK9; $p = 0.03$), positive regulation of prostaglandin biosynthetic process (MAPK9; $p = 0.019$), regulation of JNK cascade (MAPK9; $p = 0.045$), positive regulation of prostaglandin secretion (MAPK9; $p = 0.021$), positive regulation of transcription factor catabolic process (MPAK9; $p = 0.003$), JUN phosphorylation (MAPK9; $p = 0.003$), protein localization to tricellular tight junction (MAPK9; $p = 0.002$), and positive regulation of cell morphogenesis involved in differentiation (MAPK9; $p < 0.001$) (Figure S4B). Finally, MAPK9 was found to be involved in several reactome pathways in FunRich analysis such as activation of the AP-1 family of transcription factors ($p = 0.003$), FCER1 mediated MAPK activation ($p = 0.033$), and JNK (c-Jun kinases) phosphorylation and activation mediated by activated human TAK1 ($p = 0.009$) (Figure S4C).

In order to verify whether the 17 identified apoptosis proteins from cell lines were specifically stimulated in neurons following co-culture with antibody-treated microglia, we used the 'RNA expression in brain cell types' platform (<http://celltypes.org/brain/>) to measure the expression of genes in these cells (McKenzie et al., 2018). Anti-PrP antibody-treated microglia did not share any apoptotic-related proteins identified following DMT (Table S10) indicating that our 17 identified apoptosis-related proteins were specifically activated in neurons.

3.7. Contactless co-culture of Anti-PrP antibody treated-microglia N11 and N2a cell lines fails to cause apoptosis

This experiment was designed to verify whether the apoptotic effects caused by DMT were due to a direct contact or indirect release of microglial factors which in turn might have led to apoptosis. N11 cells were initially treated with ICSM18, ICSM38, POM1, POM2, POM3, SAF32, or SAF70 on tissue culture inserts before placing the inserts containing antibody treated microglia on tissue culture plate containing untreated N2a cells (IMT). IMT resulted in a final dataset of 11 proteins (9 upregulated and 2 downregulated) after LC-MS analysis. Differentially expressed proteins ($p < 0.05$) were considered with a maximum fold change ≥ 10 and at least 2 identified unique peptides and a confidence score ≥ 10 (Table S11). Of importance, functional annotation of the identified proteins following IMT did not reveal any apoptotic related proteins confirming that the antibody mediated apoptosis was due to direct cognate interaction between antibody treated N11 and N2a.

3.8. Biological confirmation of Anti-PrP related apoptosis with annexin V staining

Annexin V is a sensitive marker to detect early apoptosis (Balaji et al., 2013; Wlodkowic et al., 2009). Annexin V staining was performed following treatment with $1\mu\text{g}$ of anti-PrP antibody ICSM18 or ICSM35 then assessed with flow cytometry. Direct antibody treatment of N2a led to the significant increase of Annexin V-FITC positive cells in both ICSM18 ($p < 0.05$; 2910 ± 133) (Figure 8A) and ICSM35 ($p < 0.05$; 3223 ± 205) (Figure 8B) in comparison to the untreated cells (2833 ± 60). However, antibody treatment of the primary neuronal cells did not lead

to significant difference with untreated cells (data not shown). Furthermore, co-culture of N2a with antibody-treated N11 led to significant increase of Annexin V-FITC positive cells in both ICSM18 ($p < 0.05$; 3648 ± 143) (Figure 8C) and ICSM35 ($p < 0.05$; 4378 ± 265.2) (Figure 8D) in comparison with untreated cells (2171 ± 35.5).

Of importance, co-culture of MPN cells with antibody-treated N11 led to significant increase of Annexin V-FITC positive cells in both ICSM18 ($p < 0.05$; 1373 ± 43) (Figure 8E) and ICSM35 ($p < 0.05$; 1313 ± 65.5) (Figure 8F) in comparison with untreated cells (1060 ± 9.01). Finally, a significant increase of Annexin V-FITC positive cells was observed for both ICSM18 (1330 ± 53) (Figure 8G) and ICSM35 (1331 ± 23.5) (Figure 8H) in comparison with the 3F4 antibody treated cells (751 ± 10.3). Finally, and in order to confirm the apoptotic activity of Annexin V (positive control), N2a cells were treated with H_2O_2 (Figure S5) and led to significant increase of Annexin V-FITC positive cells in H_2O_2 -treated N2a cells ($p < 0.05$; 25000 ± 2020).

4. Discussion

In this study, we used LC-MS to investigate the detailed changes in the proteome after applying anti-PrP^C antibodies directly to neurons, or by cross-linking microglial PrP^C with anti-PrP^C antibodies prior to co-culture with neurons. We found that co-culture of neurons with anti-PrP^C antibody treated microglia led to a more substantial disturbance of the proteome.

A common but important property of all prion diseases is the conversion of a host-encoded GPI-anchored sialo-glycoprotein cellular prion protein (PrP^C), into a disease associated abnormal isoform (PrP^{Sc}), which is key to the pathogenesis of prion diseases (Prusiner, 1991; Stahl et al., 1987, 1990). White and colleagues (White et al., 2003) established the first proof of concept for antibody-based therapy for prion diseases following passive intraperitoneal administration with ICSM35 and ICSM18 antibodies produced in FVB/N *Prnp* null mice [FVB/N *Prnp*^{0/0} or Zurich I mice (Büeler et al., 1992)] against human recombinant PrP⁹¹⁻²³¹ folded either into β or α conformation respectively (Jackson et al., 1999). However, a similar PrP^C-specific antibody called D13 (Williamson et al., 1998) which binds to an epitope within the 95 to 105 region of PrP^C tail region caused extensive neurotoxicity in the hippocampus of C57BL/10 mice (Solfarosi et al., 2004). Of note, D13 was produced in PrP null mice against dispersed SHaPrP 27–30 incorporated into liposomes (Williamson et al., 1998). Klöhn and colleagues failed to reproduce the D13-mediated hippocampal neurotoxicity and appeared to demonstrate that ICSM35 was innocuous in C57BL/10 mice (Klöhn et al., 2012). A subsequent study by Reimann et al. contradicted these observations and appeared to show that D13 was indeed neurotoxic when injected to the hippocampus of C57BL/6 mice (Reimann et al., 2016). Further, these authors also showed that ICSM18 and an antibody they called POM1 raised against mouse recombinant PrP²³⁻²³¹ folded into α conformation and which binds to a discontinuous epitope within 138–147 and 204/208/212 (Polymenidou et al., 2008; Reimann et al., 2016) led to hippocampal neurotoxicity (Reimann et al., 2016). An attempt was made to justify this discrepancies by suggesting that this was due to differences of the antibody dosage (Reimann et al., 2016), however, other important factors such as differences of immunogen/antibody structure, antibody isotype, mouse strain used in the toxicity studies and more importantly the putative role played by other cellular components of the brain such as microglia were not considered. In this study, we focused on the role of anti-PrP antibody-treated microglia on neuroblastoma and primary neuronal cells toxicity by assessing the 'apoptotic proteome'. A previous study by Marella and Chabry showed that recruitment of activated microglia in the vicinity of PrP^{Sc} aggregates may cause neuronal cell damage by inducing apoptosis following direct interaction with PrP^C (Marella and Chabry, 2004). Similar to PrP^{Sc} infection, the presence of neuronal PrP^C is a *sine qua non* condition for antibody-mediated neurotoxicity *in vivo* (Reimann et al., 2016; Solfarosi et al., 2004) and *in vitro* (Tayebi et al., 2010). The antibody-mediated toxicity was intensified in

mice overexpressing PrP^C (Sonati et al., 2013), further confirming the requirement of PrP^C for this type of toxicity. In agreement with previous reports (Reimann et al., 2016), our current study confirms the neurotoxic effect of ICSM18 following direct application (DAT) of this antibody on N2a cells. Further studies on primary neuronal cells also confirmed the antibody-related apoptotic effect induced by ICSM18 and ICSM35 antibody. Although, this type of treatment (i.e. DAT) clearly led to apoptosis, the effect was limited in scope as only 4 apoptotic related proteins in N2a cells (and only 1 apoptotic related protein identified in primary neuronal cells) were identified when compared to the DMT, where 17 apoptotic related proteins (4 apoptotic related proteins identified in primary neuronal cells) were recognized; highlighting for the first time the important role played by microglia in inducing antibody-mediated toxicity. This supports the hypothesis that antibody-mediated neurotoxicity resembles the molecular pathways adopted by PrP^{Sc}-mediated neurotoxicity and is mainly caused following microglial activation and recruitment (Brown et al., 1996; Giese et al., 1998). Of note, our approach for selecting apoptotic related proteins was very stringent and relied on high-end parameters (p value ≤ 0.05 , maximum fold change ≥ 10 , unique peptide >1 , confidence score ≥ 40 –50) in comparison with the other published data where selected parameters were less stringent (e.g. low fold change values and random confidence scores) (Erin et al., 2018; Schrötter et al., 2017; Yerlikaya et al., 2015; Zafar et al., 2017; Zhao et al., 2021). Among the identified 4 apoptotic proteins (PTPRF, PAK3, RPS6KA3 and PCNT) following DAT with ICSM18, ICSM35, POM1 or SAF70 antibody, only RPS6KA3 was induced by ICSM18 antibody treatment, while PCNT was downregulated. PCNT is a large and highly conserved centrosome protein (Doxsey et al., 1994; Seo and Rhee, 2018) that binds calmodulin and mediates assembly of the mitotic spindle apparatus (Delaval and Doxsey, 2010; Flory et al., 2000; Zimmerman et al., 2004). Kim and colleagues showed that deletion of PCNT is harmful to the cells survival and also revealed that a fraction of the specific cells (Hela and U2OS) underwent apoptosis when the PCNT were deleted from the cells (Kim et al., 2019). PCNT anchoring is important for proper spindle organization and loss of the anchoring mechanism prevents mitotic entry and triggers apoptosis and cell death (Zimmerman et al., 2004). PTPRF, also known as LAR (leukocyte common antigen-related) protein (Huang et al., 2018; Stewart et al., 2017) and LAR-receptor protein tyrosine phosphatases (RTP) complex is involved in the positive regulation of the apoptosis process. RPS6KA3 which is also known as RSK2 encodes a number of RSK (ribosomal S6 kinase) family of serine/threonine kinases which play significant roles in cellular proliferation, differentiation, and cell survival (Anjum and Blenis, 2008; Carriere et al., 2008; Roux et al., 2007). The RSK family protein, especially RSK1 and RSK2, are involved in the phosphorylation and inactivation of DAPK (death-associated protein kinase) which inhibits pro-apoptotic function and increases cell survival rate in response to the mitogenic stimulation (Anjum et al., 2005; Carriere et al., 2008).

Protein-protein interaction analysis showed that PTPRF, RPS6KA3, PAK3 interact with PrP^C via MAPK3 pathway whereas PCNT interacts with PLK1 and CDC42 before networking with MAPK3 then PrP^C. MAPK3 plays a crucial role in the apoptosis signal transduction pathway through mitochondria-dependent caspase activation (Hatai et al., 2000) and mediates signal transduction of various stressors like oxidative stress as well as by receptor-mediated inflammatory signals, such as the tumour necrosis factor (TNF) or lipopolysaccharide (LPS) (Liu et al., 2000; Morita et al., 2001; Noguchi et al., 2005). In addition, the classification and gene enrichment analysis of DAT also validated the above conclusions and identified the apoptotic function of the identified proteins in which PTPRF and PAK3 are directly involved in apoptosis signal transduction pathway, whereas RPS6KA3 and PCNT are involved in the anti-apoptotic function.

DAT of primary neuronal cells when compared with untreated cells identified 1 apoptotic related protein, RSL1D1. Protein-protein interaction analysis revealed that RSL1D1 is part of the interactome that included PCNT, PTPRF, RPS6KA3, and PAK3. However, comparison of

the apoptotic profile following treatment with 3F4 antibody revealed 3 apoptotic related proteins (IKBK, SEPINA3G, and ZFP819) in DAT and 2 (ZFP819 and MAPK9) in DMT. IKBK and SERPINA3G were found in the same protein 'hub'. IKBK plays a positive regulatory role for the enhancement of apoptosis where it is proteolysed by caspases and interferes with the NF- κ B activation signals (Frelin et al., 2008). SERPINA3G is an intracellular protein and is considered as a novel EPOR/JAK2 target (Dev et al., 2014). SERPINA3G has been identified as a cytoprotective gene against oxidative stress (Dev et al., 2014; Li et al., 2014) and plays a negative regulatory role in apoptotic process and protects the cells from caspase-dependent apoptosis (Liu et al., 2003). Jin et al. showed that ZFP819 regulates the germ cell-specific gene regulation and its overexpression of ZFP819 induces apoptosis (Jin et al., 2017). Of importance, antibody-induced apoptosis following treatment with anti-PrP antibodies was confirmed through staining for Annexin V-FITC. The biological confirmation of antibody-induced apoptosis was validated in DAT and DMT of N2a cell lines as well as DMT of primary cell lines.

Our study demonstrates that DMT led to activation of 17 apoptotic related proteins in cell lines as predicted by DAVID analysis (Jiao et al., 2012). 6 out of the 17 identified proteins following DMT appeared to be downregulated while 11 were upregulated when compared to untreated control. Amongst the 6 downregulated proteins, Fibronectin type III domain-containing 1 (FNDC1) and Metallothionein 1 (MT1) are neuron-specific and not found in microglia (Hidalgo et al., 2001; Sung et al., 2011; West et al., 2008). FNDC1 is a nuclear protein involved in the positive regulation of cell apoptotic process where it initiates the apoptotic signalling in response to hypoxia (Sato et al., 2009). Metallothionein has been associated with human prion disease, bovine spongiform encephalopathy (BSE), Alzheimer's disease (AD), and multiple sclerosis (MS) (Kawashima et al., 2000; Penkowa et al., 2003; Zambenedetti et al., 1998). It was previously shown that MT3 attenuates neuronal apoptosis in the hippocampus in SAMP8 mice by increasing Bcl-2 and decreasing Bax levels (Ma et al., 2011). STRING analysis revealed that MT1 (as well as MT2 & MT3) appear to interact with PrP^C via HSP90. DOCK1, involved in cytoskeletal reorganization necessary for phagocytosis of apoptotic cells and cell motility (Wu and Horvitz, 1998) was not identified as a direct interactor with PrP^C in string analysis; however, regulation of this protein was previously shown to be intimately linked to prion incubation and progression (Majer et al., 2012) and its downregulation here suggests abnormal cytoskeletal reorganization of neurons. Cullin 7 (CUL7) is involved in the regulation of the apoptotic process (Kim et al., 2007). A study by Kim et al. showed Cul7 is an anti-apoptotic oncogene that blocks Myc-induced apoptosis in a p53-dependent manner (Kim et al., 2007). Although it was previously hypothesized that CULs, including Cul7 mediate PrP^C ubiquitination (Liu et al., 2013), we have not identified this protein as a direct interactor with PrP^C. PDE1A plays an important role in the regulation of smooth muscle cell apoptotic process and more specifically it is involved in the positive regulatory function of apoptosis (Abusnina et al., 2011; Nagel et al., 2006). PHB2, is a membrane protein involved in different cellular function including apoptosis where the mitochondrial prohibition complex controls the mitochondrial intrinsic apoptotic pathway [Reviewed in (Peng et al., 2015)]. However, its role in prion diseases is unknown but was shown to be associated with AD, Parkinson disease (PD), and Huntington's disease (HD) (Signorile et al., 2019). Interestingly, our study reveals that DMT of cell lines with POM2 led to over-expression of the highest number of apoptotic proteins ($n = 10$), followed by SAF32 ($n = 8$). Both POM2 (57–88) and SAF32 (59–89) antibodies bind to a region within the octapeptide repeat. However, the apoptotic interactome for both antibodies were variable probably due to their intrinsic properties such as isotype (IgG1 vs IgG2b), immunogen and genetic background of mice used for their production which might confer a unique conformational structure. Similarly, this was also seen with both ICSM18 and POM1 which bind to a similar globular region of PrP^C. ICSM18 induced overexpression of 8 apoptotic proteins while POM1 led to overexpression of 3 apoptotic proteins. In this case, although the isotype is similar for

both antibodies, the immunogen was distinct both in terms of the protein species (human vs mouse) and the length of the protein (truncated vs full-length). It is worth noting that a humanized version of the anti-PrP^C monoclonal antibody ICSM18 known as PRN100 did not induce apoptosis in the hippocampus of C57BL/10 mice (Klöhn et al., 2012). Another comprehensive study by Klyubin et al. found that peripheral PRN100 treatment prevents Alzheimer's disease acute A β synaptotoxicity (Klyubin et al., 2014). Although there is still debate over the neurotoxicity of ICSM18 antibody, the humanized form of ICSM18 antibody PRN100 is presently being tested in humans (Dyer, 2018). In contrast, the OR region targeting antibody POM2 was found to be neuroprotective in an *in vivo* investigation (Herrmann et al., 2015). POM2 antibody was also shown to be non-toxic in two independent studies (Reimann et al., 2016; Sonati et al., 2013). It was also discovered that POM2 as a ligand in the FT area is not only safe, but also helps reduce the toxicity of the globular domain (GD) (Herrmann et al., 2015; Sonati et al., 2013). POM2 was also shown to be capable of reducing prion-mediated neurotoxicity in tga20 cultured organotypic cerebellar slices (COCS) (Herrmann et al., 2015).

POM3 (95–100) which binds to an epitope that overlaps with ICSM35 (91–109) displayed a different apoptotic profile, probably due to the same reasons discussed above (i.e. mouse vs human and full-length vs truncated), in addition to the conformational structure of the immunogen (α -fold vs β -fold). It was previously demonstrated that ligand-specific activation of PrP^C led to a unique pattern of signalling *in vitro*. Stimulation with 6H4 anti-PrP antibody leads to alteration of MAPK signalling pathways while PrP^C activation with PrP106-126 led to activation of growth factors related signalling pathways including phosphoinositide-3 kinase (PI3K) pathway and the vascular endothelial growth factor (VEGF) signalling (Arsenault et al., 2012).

APBB1, shown to be a direct interactor with PrP^C in our study, plays a significant role in the response to DNA damage by translocating to the nucleus and inducing apoptosis and may recruit different pro-apoptosis factors such as MAPK8/JNK1 (Nakaya et al., 2008), indicating its role in antibody-mediated apoptosis.

ANK2 is composed of six helices that are very similar to the death domain of apoptotic-related proteins that seems to play a role in the auto-inhibitory functions (Wang and Lenardo, 2000). CASP8AP2 is a member of the family of cysteine proteases that contributes in the cell regulatory networks maintaining inflammation and cell death (McIlwain et al., 2015; Wang and Lenardo, 2000). However, CASP8AP2 is an initiator caspase that is associated with the proliferation of cells, and death receptor-mediated apoptosis (Wang and Lenardo, 2000). PTPRC (also known as CD45) is involved in the extrinsic apoptotic signalling pathway where the suppression of apoptosis is seen in mouse malignant T-lymphoma cells (Hanaoka et al., 1995). CUL1 is involved in the intrinsic apoptotic signalling pathway and essential for developmentally programmed transitions from the G1 phase of the cell cycle to the G0 phase or the apoptotic pathway (Kipreos et al., 1996). Sun and co-workers showed that LGMN encourages oxLDL-induced macrophage apoptosis by increasing the autophagy pathway with altered expression of Bax, caspase 3 and 9 (Sun et al., 2018). The RAG1 and RAG2 recombination assembles the immensely diverse T-cell receptor (TCR) and immunoglobulin (Ig) genes (Bassing et al., 2002; Novoa et al., 2019). *Rag1* deficient zebrafish showed increased expression of genes associated with apoptosis and greater prevalence of cell cycle arrest, apoptosis, and oxidative stress (Novoa et al., 2019). *Rag1* deficient mice were used to study the role of lymphocytes prion pathogenesis (Haybaeck et al., 2011; Onodera, 2017). RPS3 is a pro-apoptotic, ribosomal, and DNA repair endonuclease protein (Jang et al., 2004). A previous study showed that RPS3 is involved in DNA repair and helps in the induction of apoptosis through caspase dependent JNK activation (Jang et al., 2004, 2012). In the present protein-protein interaction analysis, we found that RPS3 does not interact directly with PrP^C.

Shen and co-workers reported that truncated SEMA6A induces more apoptosis than full length SEMA6A via FADD binding in lung cancer cells (Shen et al., 2018). TLR3 induces apoptosis in human breast cancer cells

through type I IFN, TRIF and molecular adapter (Salaun et al., 2006). TLR3 triggers both the intrinsic and extrinsic apoptotic signalling pathways by the activation of caspase 8 and 9 (Salaun et al., 2007; Sun et al., 2011). Of importance, IMT did not stimulate any apoptotic related proteins further proving the importance of cognate interactions of the PrP-apoptotic protein interactome.

DMT of primary neuronal cells identified 4 apoptotic related proteins (IGF1, RGCC, CHIL1, and ZFP819) when compared with untreated cells. Individual anti-PrP antibody effect analysis of 4 apoptotic proteins on primary neuronal cells when co-cultured with antibody treated N11 revealed that both ICSM18 and ICSM35 induced expression of IGF1 and RGCC.

IGF1, RGCC, CHIL1 and ZFP819 were shown to be part of the same interactome. Moreover, these proteins were also observed in the same protein 'hub' as the 17 proteins identified following DMT of cell lines, further confirming the specific apoptotic effect of the anti-PrP antibodies.

IGF-1 is well known anti-apoptotic, antioxidative, and pro-survival factor (Kim and Park, 2018; Park et al., 2012); was found to be involved in the negative regulation of apoptosis in melanoma cells (Hilmi et al., 2008), myeloma cells (Tagoug et al., 2011) and positive regulation of apoptosis in colon cancer cells (Fu et al., 2007) as well as alteration of apoptotic signalling in prostate cancer (Watson et al., 2000). Besides, IGF-1 was found to be associated with the *PRNP* gene and amyloid precursor protein (APP) expression via P13k/Akt pathway (Jiang et al., 2017). Differentially expressed RGCC was identified as an apoptotic gene in the malignant cell line U373 during the phenotypic alterations and co-cultures study (Motain et al., 2015). RGC-32 was found to be involved in the negative regulation of apoptosis including the inhibition of cell growth and invasion where RGC-32 knockdown increases the Bax, activate caspase-3, and cleaved poly (ADP-ribose) polymerase (PARP) in human lung cancer cells (Xu et al., 2014). The positive regulatory role of RGCC was established in Alzheimer's disease (AD) where RGCC reduction exhibit increasing cell survival via reduction of cdc/cyclin-dependent kinase 1 (cdk1) target cyclin B1 (Counts and Mufson, 2017).

The negative regulatory role of CHL1 has been established in inflammatory cell apoptosis through the inhibition of Fas expression, and the activation of protein kinase B/AKT (Lee et al., 2009). CHIL1 was found to be associated with prion disease mainly in the preclinical and early stages of sporadic CJD (Lorens et al., 2017; Yeo et al., 2019).

DMT of primary neuronal cells identified 2 apoptotic related proteins (ZFP819 and MAPK9) when compared with 3F4 antibody cells. MAPK contributes to the β -amyloid (A β)-induced neuronal death mechanism (Yao et al., 2005). Zinc finger protein 819 (ZFP819) is a Krüppel-associated box (KRAB) zinc finger protein family that encodes a spermatogenic cell-specific transcription factor (Jin et al., 2017) and pluripotency-related factor (Tan et al., 2013). Jin et al. showed that ZFP819 regulates the germ cell-specific gene regulation and the over-expression of ZFP819 induces the apoptosis (Jin et al., 2017). On the other hand, Tan and co-workers identified the function of ZFP819 as a novel pluripotency-related factor in genomic integrity maintenance (Tan et al., 2013).

It was speculated that the toxic effects induced by anti-PrP antibodies originate from the octapeptide repeats located in the flexible tail even when the toxic antibody binds to a motif located on the globular domain (e.g. POM1 and ICSM18) (Sonati et al., 2013). In fact, deletion of the octapeptide repeats prevented antibody-mediated toxicity directed at the globular domain (Sonati et al., 2013). Furthermore, treatment with an antibody directed at the repeats also prevented antibody-mediated toxicity directed at the globular domain (Sonati et al., 2013). Interestingly, the authors also showed that D13, which binds to an epitope outside the octapeptide repeats (95–105 region of PrP^C), if given at low dose, also prevented the toxicity of the globular domain antibodies. We have shown that a globular domain antibody (ICSM18) prevented the toxic effects of a tail domain antibody (ICSM35) (David M and Tayebi M, unpublished data), indicating that motif-specific antibody cross-linking

either the globular and/or the tail domain of PrP^C leads to apoptosis via conformational shift. However, in addition to the cross-linking effects of antibodies binding to PrP^C, additional effects such as intramolecular rearrangements, blocking of key contacts, and plasma membrane interactions of antibodies binding to PrP^C might be responsible for the possible mechanisms of toxic effects.

In conclusion and similar to PrP^{Sc}-induced apoptosis, we show that cross-linking microglial PrP^C leads to extensive toxicity of neurons. Taken together, our findings highlight the importance of investigating the role of antibody toxicity via microglia in other related neurodegenerative diseases such as AD.

Declarations

Author contribution statement

Utpal Kumar Adhikari: Performed the experiments; Analyzed and interpreted the data; Wrote the paper.

Elif Sakiz, Umma Habiba, Meena Mikhael, Matteo Senesi: Performed the experiments.

Monique Antoinette David, Gilles J. Guillemain, Lezanne Ooi, Tim Karl, Steven Collins: Contributed reagents, materials, analysis tools or data; Wrote the paper.

Mourad Tayebi: Conceived and designed the experiments; Analyzed and interpreted the data; Wrote the paper.

Funding statement

This work was supported by an Ainsworth Medical Research Innovation Fund Grant awarded to Mourad Tayebi.

Utpal Kumar Adhikari was awarded an Australian Government Research Training Program Stipend Scholarship (RTP) for PhD support.

Data availability statement

Data included in article/supplementary material/referenced in article.

Declaration of interests statement

The authors declare no conflict of interest.

Additional information

Supplementary content related to this article has been published online at <https://doi.org/10.1016/j.heliyon.2021.e08644>.

References

- Abusnina, A., Alhosin, M., Keravis, T., Muller, C.D., Fuhrmann, G., Bronner, C., Lugnier, C., 2011. Down-regulation of cyclic nucleotide phosphodiesterase PDE1A is the key event of p73 and UHRF1 deregulation in thymoquinone-induced acute lymphoblastic leukemia cell apoptosis. *Cell. Signal.* 23, 152–160.
- Adjou, K.T., Demaimay, R., Lasmézas, C., Deslys, J.P., Seman, M., Dormont, D., 1995. MS-8209, a new amphotericin B derivative, provides enhanced efficacy in delaying hamster scrapie. *Antimicrob. Agents Chemother.* 39, 2810–2812.
- Adjou, K.T., Demaimay, R., Lasmézas, C.I., Seman, M., Deslys, J.P., Dormont, D., 1996. Differential effects of a new amphotericin B derivative, MS-8209, on mouse BSE and scrapie: implications for the mechanism of action of polyene antibiotics. *Res. Virol.* 147, 213–218.
- Adjou, K.T., Privat, N., Demart, S., Deslys, J.-P., Seman, M., Hauw, J.-J., Dormont, D., 2000. MS-8209, an amphotericin B Analogue, Delays the appearance of spongiosis, astrogliosis and PrPres accumulation in the brain of scrapie-infected hamsters. *J. Comp. Pathol.* 122, 3–8.
- Aguzzi, A., Falsig, J., 2012. Prion propagation, toxicity and degradation. *Nat. Neurosci.* 15, 936–939.
- Aguzzi, A., Zhu, C., 2017. Microglia in prion diseases. *J. Clin. Invest.* 127, 3230–3239.

- Andrade, V., Guerra, M., Jardim, C., Melo, F., Silva, W., Ortega, J.M., Robert, M., Nathanson, M.H., Leite, F., 2011. Nucleoplasmic calcium regulates cell proliferation through legumain. *J. Hepatol.* 55, 626–635.
- Anjum, R., Blenis, J., 2008. The RSK family of kinases: emerging roles in cellular signalling. *Nat. Rev. Mol. Cell Biol.* 9, 747–758.
- Anjum, R., Roux, P.P., Ballif, B.A., Gygi, S.P., Blenis, J., 2005. The tumor suppressor DAP kinase is a target of RSK-mediated survival signaling. *Curr. Biol.* 15, 1762–1767.
- Arsenault, R.J., Li, Y., Potter, A., Griebel, P.J., Kusalik, A., Napper, S., 2012. Induction of ligand-specific PrP (C) signaling in human neuronal cells. *Prion* 6, 477–488.
- Baker, C.A., Martin, D., Manuelidis, L., 2002. Microglia from Creutzfeldt-Jakob disease-infected brains are infectious and show specific mRNA activation profiles. *J. Virol.* 76, 10905–10913.
- Balaji, N., Devy, A.S., Sumathi, M.K., Vidyalakshmi, S., Kumar, G.S., D'Silva, S., 2013. Annexin v - affinity assay - apoptosis detection system in granular cell ameloblastoma. *J. Int. Oral Health* 5, 25–30.
- Bardelli, M., Frontzek, K., Simonelli, L., Hornemann, S., Pedotti, M., Mazzola, F., Carta, M., Eckhardt, V., D'Antuono, R., Virgilio, T., et al., 2018. A bispecific immunotweezer prevents soluble PrP oligomers and abolishes prion toxicity. *PLoS Pathog.* 14, e1007335.
- Bassing, C.H., Swat, W., Alt, F.W., 2002. The mechanism and regulation of chromosomal V(D)J recombination. *Cell* 109 (Suppl), S45–55.
- Bera, R., Chiou, C.-Y., Yu, M.-C., Peng, J.-M., He, C.-R., Hsu, C.-Y., Huang, H.-L., Ho, U.-Y., Lin, S.-M., Lin, Y.-J., et al., 2014. Functional genomics identified a novel protein tyrosine phosphatase receptor type F-mediated growth inhibition in hepatocarcinogenesis. *Hepatology* 59, 2238–2250.
- Beringue, V., Mallinson, G., Kaiser, M., Tayebi, M., Sattar, Z., Jackson, G., Anstee, D., Collinge, J., Hawke, S., 2003. Regional heterogeneity of cellular prion protein isoforms in the mouse brain. *Brain: J. Neurol.* 126, 2065–2073.
- Brown, D.R., Schmidt, B., Kretzschmar, H.A., 1996. Role of microglia and host prion protein in neurotoxicity of a prion protein fragment. *Nature* 380, 345–347.
- Büeler, H., Fischer, M., Lang, Y., Bluethmann, H., Lipp, H.P., DeArmond, S.J., Prusiner, S.B., Aguet, M., Weissmann, C., 1992. Normal development and behaviour of mice lacking the neuronal cell-surface PrP protein. *Nature* 356, 577–582.
- Carriere, A., Ray, H., Blenis, J., Roux, P.P., 2008. The RSK factors of activating the Ras/MAPK signaling cascade. *Front. Biosci. J. Vis. Literacy* 13, 4258–4275.
- Caughey, B., Raymond, G.J., 1993. Sulfated polyanion inhibition of scrapie-associated PrP accumulation in cultured cells. *J. Virol.* 67, 643–650.
- Counts, S.E., Mufson, E.J., 2017. Regulator of cell cycle (RGCC) expression during the progression of Alzheimer's disease. *Cell Transplant.* 26, 693–702.
- Delaval, B., Dooxey, S.J., 2010. Pericentrin in cellular function and disease. *J. Cell Biol.* 188, 181–190.
- Demart, S., Fournier, J.-G., Creminon, C., Frobert, Y., Lamoury, F., Marce, D., Lasmézas, C., Dormont, D., Grassi, J., Deslys, J.-P., 1999. New insight into abnormal prion protein using monoclonal antibodies. *Biochem. Biophys. Res. Commun.* 265, 652–657.
- Dev, A., Byrne, S.M., Verma, R., Ashton-Rickardt, P.G., Wojchowski, D.M., 2014. Erythropoietin-directed erythropoiesis depends on serpin inhibition of erythroblast lysosomal cathepsins. *J. Exp. Med.* 211, 381.
- Dooxey, S.J., Stein, P., Evans, L., Calarco, P.D., Kirschner, M., 1994. Pericentrin, a highly conserved centrosome protein involved in microtubule organization. *Cell* 76, 639–650.
- Dyer, C., 2018. British man with CJD gets experimental treatment in world first. *Br. Med. J.* 363, k4608.
- Ehlers, B., Diringer, H., 1984. Dextran sulphate 500 delays and prevents mouse scrapie by impairment of agent replication in spleen. *J. Gen. Virol.* 65 (Pt 8), 1325–1330.
- Enari, M., Flechsig, E., Weissmann, C., 2001. Scrapie prion protein accumulation by scrapie-infected neuroblastoma cells abrogated by exposure to a prion protein antibody. *Proc. Natl. Acad. Sci. U.S.A.* 98, 9295–9299.
- Endo, T., Groth, D., Prusiner, S.B., Kobata, A., 1989. Diversity of oligosaccharide structures linked to asparagines of the scrapie prion protein. *Biochemistry* 28, 8380–8388.
- Erin, N., Ogan, N., Yerlikaya, A., 2018. Secretomes reveal several novel proteins as well as TGF-β1 as the top upstream regulator of metastatic process in breast cancer. *Breast Cancer Res. Treat.* 170, 235–250.
- Felton, L.M., Cunningham, C., Rankine, E.L., Waters, S., Boche, D., Perry, V.H., 2005. MCP-1 and murine prion disease: separation of early behavioural dysfunction from overt clinical disease. *Neurobiol. Dis.* 20, 283–295.
- Féraudet, C., Morel, N., Simon, S., Volland, H., Frobert, Y., Créminon, C., Vilette, D., Lehmann, S., Grassi, J., 2005. Screening of 145 anti-PrP monoclonal antibodies for their capacity to inhibit PrP^{Sc} replication in infected cells. *J. Biol. Chem.* 280, 11247–11258.
- Flory, M.R., Moser, M.J., Monnat, R.J.J., Davis, T.N., 2000. Identification of a human centrosomal calmodulin-binding protein that shares homology with pericentrin. *Proc. Natl. Acad. Sci. U.S.A.* 97, 5919–5923.
- Forloni, G., Iussich, S., Awan, T., Colombo, L., Angeretti, N., Girola, L., Bertani, I., Poli, G., Caramelli, M., Grazia Bruzzone, M., et al., 2002. Tetracyclines affect prion infectivity. *Proc. Natl. Acad. Sci. U.S.A.* 99, 10849–10854.
- Frelin, C., Imbert, V., Bottero, V., Gonthier, N., Samraj, A.K., Schulze-Osthoff, K., Auberger, P., Courtois, G., Peyron, J.-F., 2008. Inhibition of the NF-κB survival pathway via caspase-dependent cleavage of the IKK complex scaffold protein and NF-κB essential modulator NEMO. *Cell Death Differ.* 15, 152–160.
- Fu, P., Thompson, J.A., Leeding, K.S., Bach, L.A., 2007. Insulin-like growth factors induce apoptosis as well as proliferation in LIM 1215 colon cancer cells. *J. Cell. Biochem.* 100, 58–68.

- Giese, A., Brown, D.R., Groschup, M.H., Feldmann, C., Haist, I., Kretschmar, H.A., 1998. Role of microglia in neuronal cell death in prion disease. *Brain Pathol.* 8, 449–457.
- Haigh, C.L., McGlade, A.R., Lewis, V., Masters, C.L., Lawson, V.A., Collins, S.J., 2011. Acute exposure to prion infective induces transient oxidative stress progressing to be cumulatively deleterious with chronic propagation in vitro. *Free Radic. Biol. Med.* 51, 594–608.
- Hanaoka, K., Fujita, N., Lee, S.H., Seimiya, H., Naito, M., Tsuruo, T., 1995. Involvement of CD45 in adhesion and suppression of apoptosis of mouse malignant T-lymphoma cells. *Cancer Res.* 55, 2186–2190.
- Hanayama, R., Tanaka, M., Miwa, K., Shinohara, A., Iwamoto, A., Nagata, S., 2002. Identification of a factor that links apoptotic cells to phagocytes. *Nature* 417, 182–187.
- Haraguchi, T., Fisher, S., Olofsson, S., Endo, T., Groth, D., Tarentino, A., Borchelt, D.R., Teplow, D., Hood, L., Burlingame, A., et al., 1989. Asparagine-linked glycosylation of the scrapie and cellular prion proteins. *Arch. Biochem. Biophys.* 274, 1–13.
- Hata, T., Nakayama, M., 2007. Targeted disruption of the murine large nuclear KIAA1440/Ints1 protein causes growth arrest in early blastocyst stage embryos and eventual apoptotic cell death. *Biochim. Biophys. Acta Mol. Cell Res.* 1773, 1039–1051.
- Hatai, T., Matsuzawa, A., Inoshita, S., Mochida, Y., Kuroda, T., Sakamaki, K., Kuida, K., Yonehara, S., Ichijo, H., Takeda, K., 2000. Execution of apoptosis signal-regulating kinase 1 (ASK1)-induced apoptosis by the mitochondria-dependent caspase activation. *J. Biol. Chem.* 275, 26576–26581.
- Haybaeck, J., Heikenwalder, M., Klevenz, B., Schwarz, P., Margalith, I., Bridel, C., Mertz, K., Zirdum, E., Petsch, B., Fuchs, T.J., et al., 2011. Aerosols transmit prions to immunocompetent and immunodeficient mice. *PLoS Pathog.* 7, e1001257.
- Heppner, F.L., Musahl, C., Arrighi, I., Klein, M.A., Rüllicke, T., Oesch, B., Zinkernagel, R.M., Kalinke, U., Aguzzi, A., 2001. Prevention of scrapie pathogenesis by transgenic expression of anti-prion protein antibodies. *Science* 294, 178–182.
- Herrmann, U.S., Sonati, T., Falsig, J., Reimann, R.R., Dametto, P., O'Connor, T., Li, B., Lau, A., Hornemann, S., Sorce, S., et al., 2015. Prion infections and anti-PrP antibodies trigger converging neurotoxic pathways. *PLoS Pathog.* 11, e1004662.
- Hidalgo, J., Aschner, M., Zatta, P., Vašák, M., 2001. Roles of the metallothionein family of proteins in the central nervous system. *Brain Res. Bull.* 55, 133–145.
- Hilmi, C., Larrrière, L., Giuliano, S., Bille, K., Ortonne, J.-P., Ballotti, R., Bertolotto, C., 2008. IGF1 promotes resistance to apoptosis in melanoma cells through an increased expression of BCL2, BCL-XL, and survivin. *J. Invest. Dermatol.* 128, 1499–1505.
- Huang, D.W., Sherman, B.T., Lempicki, R.A., 2009. Systematic and integrative analysis of large gene lists using DAVID bioinformatics resources. *Nat. Protoc.* 4, 44–57.
- Huang, Y., Zhang, Y., Ge, L., Lin, Y., Kwok, H.F., 2018. The roles of protein tyrosine phosphatases in hepatocellular carcinoma. *Cancers* 10.
- Jackson, G.S., Hill, A.F., Joseph, C., Hosszu, L., Power, A., Walther, J.P., Clarke, A.R., Collinge, J., 1999. Multiple folding pathways for heterologously expressed human prion protein. *Biochim. Biophys. Acta Protein Struct. Mol. Enzymol.* 1431, 1–13.
- Jang, C.-Y., Lee, J.Y., Kim, J., 2004. Rps3, a DNA repair endonuclease and ribosomal protein, is involved in apoptosis. *FEBS (Fed. Eur. Biochem. Soc.) Lett.* 560, 81–85.
- Jang, C.-Y., Kim, H.D., Kim, J., 2012. Ribosomal protein S3 interacts with TRADD to induce apoptosis through caspase dependent JNK activation. *Biochem. Biophys. Res. Commun.* 421, 474–478.
- Jiang, G., Wang, C., Zhang, J., Liu, H., 2017. Mediation of insulin growth factor-1 in Alzheimer's disease and the mechanism of PRNP genetic expression and the PI3K/Akt signaling pathway. *Exp. Ther. Med.* 13, 2763–2766.
- Jiao, X., Sherman, B.T., Huang, D.W., Stephens, R., Baseler, M.W., Lane, H.C., Lempicki, R.A., 2012. DAVID-WS: a stateful web service to facilitate gene/protein list analysis. *Bioinformatics* 28, 1805–1806.
- Jin, S., Choi, H., Kwon, J.T., Kim, J., Jeong, J., Kim, J., Hong, S.H., Cho, C., 2017. Identification of target genes for spermatogenic cell-specific KRAB transcription factor ZFP819 in a male germ cell line. *Cell Biosci.* 7, 4.
- Jones, D.R., Taylor, W.A., Bate, C., David, M., Tayebi, M., 2010. A camelid anti-PrP antibody abrogates PrP replication in prion-permissive neuroblastoma cell lines. *PLoS One* 5, e9804 e9804.
- Kascasak, R.J., Rubenstein, R., Merz, P.A., Tonna-DeMasi, M., Fersko, R., Carp, R.I., Wisniewski, H.M., Diringer, H., 1987. Mouse polyclonal and monoclonal antibody to scrapie-associated fibril proteins. *J. Virol.* 61, 3688–3693.
- Kawashima, T., Doh-ura, K., Torisu, M., Uchida, Y., Furuta, A., Iwaki, T., 2000. Differential expression of metallothioneins in human prion diseases. *Dement. Geriatr. Cognit. Disord.* 11, 251–262.
- Kim, C., Park, S., 2018. IGF-1 protects SH-SY5Y cells against MPP+ induced apoptosis via PI3K/PDK1/Akt pathway. *Endocrine Connect.* 7, 443–455.
- Kim, J., Kim, J., Rhee, K., 2019. PCNT is critical for the association and conversion of centrosomes to centrosomes during mitosis. *J. Cell Sci.* 132.
- Kim, S.S., Shago, M., Kaustov, L., Boutros, P.C., Clendenning, J.W., Sheng, Y., Trentin, G.A., Barsyte-Lovejoy, D., Mao, D.Y.L., Kay, R., et al., 2007. CUL7 is a novel antiapoptotic oncogene. *Cancer Res.* 67, 9616–9622.
- Kipreos, E.T., Lander, L.E., Wing, J.P., He, W.W., Hedgecock, E.M., 1996. cul-1 is required for cell cycle exit in *C. elegans* and identifies a novel gene family. *Cell* 85, 829–839.
- Klebe, R.J., 1969. Neuroblastoma: cell culture analysis of a differentiating stem cell system. *J. Cell Biol.* 43, 69A.
- Klöhn, P.-C., Farmer, M., Linehan, J.M., O'Malley, C., de Marco, M., Taylor, W., Farrow, M., Khalili-Shirazi, A., Brandner, S., Collinge, J., 2012. PrP antibodies do not trigger mouse hippocampal neuron apoptosis. *Science (New York, N.Y.)* 335, 52.
- Klyubin, I., Nicoll, A.J., Khalili-Shirazi, A., Farmer, M., Canning, S., Mably, A., Linehan, J., Brown, A., Wakeling, M., Brandner, S., et al., 2014. Peripheral administration of a humanized anti-PrP antibody blocks Alzheimer's disease A β synaptotoxicity. *J. Neurosci. : Off. J. Soc. Neurosci.* 34, 6140–6145.
- Korth, C., May, B.C., Cohen, F.E., Prusiner, S.B., 2001. Acridine and phenothiazine derivatives as pharmacotherapeutics for prion disease. *Proc. Natl. Acad. Sci. U.S.A.* 98, 9836–9841.
- Lee, C.G., Hartl, D., Lee, G.R., Koller, B., Matsuura, H., Da Silva, C.A., Sohn, M.H., Cohn, L., Homer, R.J., Kozhich, A.A., et al., 2009. Role of breast regression protein 39 (BRP-39)/chitinase 3-like-1 in Th2 and IL-13-induced tissue responses and apoptosis. *J. Exp. Med.* 206, 1149–1166.
- Li, L., Byrne, S.M., Rainville, N., Su, S., Jachimowicz, E., Aucher, A., Davis, D.M., Ashton-Rickardt, P.G., Wojchowski, D.M., 2014. Brief report: serpin Spi2A as a novel modulator of hematopoietic progenitor cell formation. *Stem Cell.* 32, 2550–2556.
- Li, N., Zhao, G., Chen, T., Xue, L., Ma, L., Niu, J., Tong, T., 2012. Nucleolar protein CSIG is required for p33ING1 function in UV-induced apoptosis. *Cell Death Dis.* 3, e283 e283.
- Liu, H., Nishitoh, H., Ichijo, H., Kyriakis, J.M., 2000. Activation of apoptosis signal-regulating kinase 1 (ASK1) by tumor necrosis factor receptor-associated factor 2 requires prior dissociation of the ASK1 inhibitor thioredoxin. *Mol. Cell Biol.* 20, 2198–2208.
- Liu, N., Raja, S.M., Zazzeroni, F., Metkar, S.S., Shah, R., Zhang, M., Wang, Y., Brömme, D., Russin, W.A., Lee, J.C., et al., 2003. NF-kappaB protects from the lysosomal pathway of cell death. *EMBO J.* 22, 5313–5322.
- Liu, Z., Xiang, Y., Sun, G., 2013. The KCTD family of proteins: structure, function, disease relevance. *Cell Biosci.* 3, 45.
- Llorens, F., Thüne, K., Tahir, W., Kanata, E., Diaz-Lucena, D., Xanthopoulos, K., Kovatsi, E., Pleschka, C., Garcia-Esparcia, P., Schmitz, M., et al., 2017. YKL-40 in the brain and cerebrospinal fluid of neurodegenerative dementias. *Mol. Neurodegener.* 12, 83.
- Lv, Y., Chen, C., Zhang, B.-Y., Xiao, K., Wang, J., Chen, L.-N., Sun, J., Gao, C., Shi, Q., Dong, X.-P., 2015. Remarkable activation of the complement system and aberrant neuronal localization of the membrane attack complex in the brain tissues of scrapie-infected rodents. *Mol. Neurobiol.* 52, 1165–1179.
- Ma, F., Wang, H., Chen, B., Wang, F., Xu, H., 2011. Metallothionein 3 attenuated the apoptosis of neurons in the CA1 region of the hippocampus in the senescence-accelerated mouse/PRONE8 (SAMP8). *Arq. Neuro. Psychiatr.* 69, 105–111.
- Ma, L., Zhao, W., Zhu, F., Yuan, F., Xie, N., Li, T., Wang, P., Tong, T., 2015. Global characteristics of CSIG-associated gene expression changes in human HEK293 cells and the implications for CSIG regulating cell proliferation and senescence. *Front. Endocrinol.* 6, 69.
- Majer, A., Medina, S.J., Niu, Y., Abrenica, B., Manguiat, K.J., Frost, K.L., Philipson, C.S., Sorensen, D.L., Booth, S.A., 2012. Early mechanisms of pathobiology are revealed by transcriptional temporal dynamics in hippocampal CA1 neurons of prion infected mice. *PLoS Pathog.* 8, e1003002.
- Marella, M., Chabry, J., 2004. Neurons and astrocytes respond to prion infection by inducing microglia recruitment. *J. Neurosci. Off. J. Soc. Neurosci.* 24, 620–627.
- Mazzoni, I.E., Ledebur, H.C.J., Paramithiotis, E., Cashman, N., 2005. Lymphoid signal transduction mechanisms linked to cellular prion protein. *Biochem. Cell. Biol.* 83, 644–653.
- McIlwain, D.R., Berger, T., Mak, T.W., 2015. Caspase functions in cell death and disease. *Cold Spring Harbor Perspect. Biol.* 7.
- McKenzie, A.T., Wang, M., Hauberg, M.E., Fullard, J.F., Kozlenkov, A., Keenan, A., Hurd, Y.L., Dracheva, S., Casaccia, P., Roussos, P., et al., 2018. Brain cell type specific gene expression and Co-expression network architectures. *Sci. Rep.* 8, 8868.
- McPhie, D.L., Coopersmith, R., Hines-Peralta, A., Chen, Y., Ivins, K.J., Manly, S.P., Kozlowski, M.R., Neve, K.A., Neve, R.L., 2003. DNA synthesis and neuronal apoptosis caused by familial Alzheimer disease mutants of the amyloid precursor protein are mediated by the p21 activated kinase PAK3. *J. Neurosci. Off. J. Soc. Neurosci.* 23, 6914–6927.
- Mi, H., Muruganujan, A., Huang, X., Ebert, D., Mills, C., Guo, X., Thomas, P.D., 2019. Protocol Update for large-scale genome and gene function analysis with the PANTHER classification system (v.14.0). *Nat. Protoc.* 14, 703–721.
- Mok, S.W.F., Riemer, C., Madela, K., Hsu, D.K., Liu, F.-T., Gültner, S., Heise, I., Baier, M., 2007. Role of galectin-3 in prion infections of the CNS. *Biochem. Biophys. Res. Commun.* 359, 672–678.
- Monzón, M., Hernández, R.S., Garcés, M., Sarasa, R., Badiola, J.J., 2018. Glial alterations in human prion diseases: a correlative study of astroglia, reactive microglia, protein deposition, and neuropathological lesions. *Medicine* 97, e0320.
- Morita, K., Saitoh, M., Tobiume, K., Matsuura, H., Enomoto, S., Nishitoh, H., Ichijo, H., 2001. Negative feedback regulation of ASK1 by protein phosphatase 5 (PP5) in response to oxidative stress. *EMBO J.* 20, 6028–6036.
- Motaln, H., Koren, A., Gruden, K., Ramsak, Z., Schichor, C., Lah, T.T., 2015. Heterogeneous glioblastoma cell cross-talk promotes phenotype alterations and enhanced drug resistance. *Oncotarget* 6, 40998–41017.
- Mouillet-Richard, S., Ermonval, M., Chebassier, C., Laplanche, J.L., Lehmann, S., Launay, J.M., Kellermann, O., 2000. Signal transduction through prion protein. *Science* 289, 1925–1928.
- Nagel, D.J., Aizawa, T., Jeon, K.-I., Liu, W., Mohan, A., Wei, H., Miano, J.M., Florio, V.A., Gao, P., Korshunov, V.A., et al., 2006. Role of nuclear Ca²⁺/calmodulin-stimulated phosphodiesterase 1A in vascular smooth muscle cell growth and survival. *Circ. Res.* 98, 777–784.
- Nakaya, T., Kawai, T., Suzuki, T., 2008. Regulation of FE65 nuclear translocation and function by amyloid beta-protein precursor in osmotically stressed cells. *J. Biol. Chem.* 283, 19119–19131.

- N'Diaye, E.-N., Branda, C.S., Branda, S.S., Nevarez, L., Colonna, M., Lowell, C., Hamerman, J.A., Seaman, W.E., 2009. TREM-2 (triggering receptor expressed on myeloid cells 2) is a phagocytic receptor for bacteria. *J. Cell Biol.* 184, 215–223.
- Noguchi, T., Takeda, K., Matsuzawa, A., Saegusa, K., Nakano, H., Gohda, J., Inoue, J.-I., Ichijo, H., 2005. Recruitment of tumor necrosis factor receptor-associated factor family proteins to apoptosis signal-regulating kinase 1 signalosome is essential for oxidative stress-induced cell death. *J. Biol. Chem.* 280, 37033–37040.
- Novoa, B., Pereiro, P., López-Muñoz, A., Varela, M., Forn-Cuní, G., Anhelín, M., Dios, S., Romero, A., Martínez-López, A., Medina-Gali, R.M., et al., 2019. Rgl1 immunodeficiency-induced early aging and senescence in zebrafish are dependent on chronic inflammation and oxidative stress. *Aging Cell* 18, e13020.
- Onodera, T., 2017. Dual role of cellular prion protein in normal host and Alzheimer's disease. *Proc. Jpn. Acad. B Phys. Biol. Sci.* 93, 155–173.
- Pankiewicz, J., Prelli, F., Sy, M.-S., Kasczak, R.J., Kasczak, R.B., Spinner, D.S., Carp, R.I., Meeker, H.C., Sadowski, M., Wisniewski, T., 2006. Clearance and prevention of prion infection in cell culture by anti-PrP antibodies. *Eur. J. Neurosci.* 23, 2635–2647.
- Park, Y.-G., Jeong, J.-K., Moon, M.-H., Lee, J.-H., Lee, Y.-J., Seol, J.-W., Kim, S.-J., Kang, S.-J., Park, S.-Y., 2012. Insulin-like growth factor-1 protects against prion peptide-induced cell death in neuronal cells via inhibition of Bax translocation. *Int. J. Mol. Med.* 30, 1069–1074.
- Pathan, M., Keerthikumar, S., Ang, C.-S., Gangoda, L., Quek, C.Y.J., Williamson, N.A., Mouradov, D., Sieber, O.M., Simpson, R.J., Salim, A., et al., 2015. FunRich: an open access standalone functional enrichment and interaction network analysis tool. *Proteomics* 15, 2597–2601.
- Pathan, M., Keerthikumar, S., Chisanga, D., Alessandro, R., Ang, C.-S., Askenase, P., Batagov, A.O., Benito-Martin, A., Camussi, G., Clayton, A., et al., 2017. A novel community driven software for functional enrichment analysis of extracellular vesicles data. *J. Extracell. Vesicles* 6, 1321455.
- Peng, Y.-T., Chen, P., Ouyang, R.-Y., Song, L., 2015. Multifaceted role of prohibitin in cell survival and apoptosis. *Apoptosis: Int. J. Program. Cell Death* 20, 1135–1149.
- Penkowa, M., Espejo, C., Ortega-Aznar, A., Hidalgo, J., Montalban, X., Martínez Cáceres, E.M., 2003. Metallothionein expression in the central nervous system of multiple sclerosis patients. *Cell. Mol. Life Sci. CMLS* 60, 1258–1266.
- Polymenidou, M., Moos, R., Scott, M., Sigurdson, C., Shi, Y.-Z., Yajima, B., Hafner-Bratkovic, I., Jerala, R., Hornemann, S., Wuthrich, K., et al., 2008. The POM monoclonals: a comprehensive set of antibodies to non-overlapping prion protein epitopes. *PLoS One* 3, e3872.
- Prusiner, S.B., 1991. Molecular biology of prion diseases. *Science (New York, N.Y.)* 252, 1515–1522.
- Prusiner, S.B., DeArmond, S.J., 1994. Prion diseases and neurodegeneration. *Annu. Rev. Neurosci.* 17, 311–339.
- Reimann, R.R., Sonati, T., Hornemann, S., Herrmann, U.S., Arand, M., Hawke, S., Aguzzi, A., 2016. Differential toxicity of antibodies to the prion protein. *PLoS Pathog.* 12, e1005401 e1005401.
- Righi, M., Mori, L., Libero, G. De, Sironi, M., Biondi, A., Mantovani, A., Donini, S.D., Ricciardi-Castagnoli, P., 1989. Monokine production by microglial cell clones. *Eur. J. Immunol.* 19, 1443–1448.
- Roux, P.P., Shabbazian, D., Vu, H., Holz, M.K., Cohen, M.S., Taunton, J., Sonenberg, N., Blenis, J., 2007. RAS/ERK signaling promotes site-specific ribosomal protein S6 phosphorylation via RSK and stimulates cap-dependent translation. *J. Biol. Chem.* 282, 14056–14064.
- Salaun, B., Coste, I., Risoan, M.-C., Lebecque, S.J., Renno, T., 2006. TLR3 can directly trigger apoptosis in human cancer cells. *J. Immunol.* 176, 4894–4901 (Baltimore, Md. : 1950).
- Salaun, B., Lebecque, S., Matikainen, S., Rimoldi, D., Romero, P., 2007. Toll-like receptor 3 expressed by melanoma cells as a target for therapy? *Clin. Cancer Res. Off. J. Am. Assoc. Cancer Res.* 13, 4565–4574.
- Sato, M., Jiao, Q., Honda, T., Kurotani, R., Toyota, E., Okumura, S., Takeya, T., Minamisawa, S., Lanier, S.M., Ishikawa, Y., 2009. Activator of G protein signaling 8 (AGS8) is required for hypoxia-induced apoptosis of cardiomyocytes: role of G betagamma and connexin 43 (CX43). *J. Biol. Chem.* 284, 31431–31440.
- Schrötter, A., Oberhaus, A., Kolbe, K., Seger, S., Mastalski, T., El Magraoui, F., Hoffmann-Porsorske, E., Bohnert, M., Deckert, J., Braun, C., et al., 2017. LMD proteomics provides evidence for hippocampus field-specific motor protein abundance changes with relevance to Alzheimer's disease. *Biochim. Biophys. Acta Protein Proteomics* 1865, 703–714.
- Schultz, J., Schwarz, A., Neidhold, S., Burwinkel, M., Riemer, C., Simon, D., Kopf, M., Otto, M., Baier, M., 2004. Role of interleukin-1 in prion disease-associated astrocyte activation. *Am. J. Pathol.* 165, 671–678.
- Schwarz, A., Krätke, O., Burwinkel, M., Riemer, C., Schultz, J., Henklein, P., Bamme, T., Baier, M., 2003. Immunisation with a synthetic prion protein-derived peptide prolongs survival times of mice orally exposed to the scrapie agent. *Neurosci. Lett.* 350, 187–189.
- Seo, M.Y., Rhee, K., 2018. Caspase-mediated cleavage of the centrosomal proteins during apoptosis. *Cell Death Dis.* 9, 571.
- Sethi, S., Lipford, G., Wagner, H., Kretschmar, H., 2002. Postexposure prophylaxis against prion disease with a stimulator of innate immunity. *Lancet* 360, 229–230.
- Shen, C.-Y., Chang, Y.-C., Chen, L.-H., Lin, W.-C., Lee, Y.-H., Yeh, S.-T., Chen, H.-K., Fang, W., Hsu, C.-P., Lee, J.-M., et al., 2018. The extracellular SEMA domain attenuates intracellular apoptotic signaling of semaphorin 6A in lung cancer cells. *Oncogenesis* 7, 95.
- Shimoda, R., Achanzar, W.E., Qu, W., Nagamine, T., Takagi, H., Mori, M., Waalkes, M.P., 2003. Metallothionein is a potential negative regulator of apoptosis. *Toxicol. Sci. : Off. J. Soc. Toxicol.* 73, 294–300.
- Signorile, A., Sgaramella, G., Bellomo, F., De Rasmio, D., 2019. Prohibitins: a critical role in mitochondrial functions and implication in diseases. *Cells* 8.
- Sigurdsson, E.M., Brown, D.R., Daniels, M., Kasczak, R.J., Kasczak, R., Carp, R., Meeker, H.C., Frangione, B., Wisniewski, T., 2002. Immunization delays the onset of prion disease in mice. *Am. J. Pathol.* 161, 13–17.
- Solfrosi, L., Criado, J.R., McGavern, D.B., Wirz, S., Sánchez-Alavez, M., Sugama, S., DeGiorgio, L.A., Volpe, B.T., Wiseman, E., Abalos, G., et al., 2004. Cross-linking cellular prion protein triggers neuronal apoptosis in vivo. *Science (New York, N.Y.)* 303, 1514–1516.
- Sonati, T., Reimann, R.R., Falsig, J., Baral, P.K., O'Connor, T., Hornemann, S., Yaganoglu, S., Li, B., Herrmann, U.S., Wieland, B., et al., 2013. The toxicity of anti-prion antibodies is mediated by the flexible tail of the prion protein. *Nature* 501, 102.
- Soto, C., Kasczak, R.J., Saborío, G.P., Aucouturier, P., Wisniewski, T., Prelli, F., Kasczak, R., Mendez, E., Harris, D.A., Ironside, J., et al., 2000. Reversion of prion protein conformational changes by synthetic b-sheet breaker peptides. *Lancet* 355, 192–197.
- Stahl, N., Borchelt, D.R., Hsiao, K., Prusiner, S.B., 1987. Scrapie prion protein contains a phosphatidylinositol glycolipid. *Cell* 51, 229–240.
- Stahl, N., Borchelt, D.R., Prusiner, S.B., 1990. Differential release of cellular and scrapie prion proteins from cellular membranes by phosphatidylinositol-specific phospholipase C. *Biochemistry* 29, 5405–5412.
- Stewart, K., Tang, Y.C., Shafer, M.E.R., Graham-Paquin, A.-L., Bouchard, M., 2017. Modulation of apoptotic response by LAR family phosphatases-clAP1 signaling during urinary tract morphogenesis. *Proc. Natl. Acad. Sci. U.S.A.* 114, E9016–E9025.
- Sun, R., Zhang, Y., Lv, Q., Liu, B., Jin, M., Zhang, W., He, Q., Deng, M., Liu, X., Li, G., et al., 2011. Toll-like receptor 3 (TLR3) induces apoptosis via death receptors and mitochondria by up-regulating the transactivating p63 isoform alpha (TAP63alpha). *J. Biol. Chem.* 286, 15918–15928.
- Sun, W., Lin, Y., Chen, L., Ma, R., Cao, J., Yao, J., Chen, K., Wan, J., 2018. Legumain suppresses OxLDL-induced macrophage apoptosis through enhancement of the autophagy pathway. *Gene* 652, 16–24.
- Sung, C.O., Kim, S.C., Karnan, S., Karube, K., Shin, H.J., Nam, D.-H., Suh, Y.-L., Kim, S.-H., Kim, J.Y., Kim, S.J., et al., 2011. Genomic profiling combined with gene expression profiling in primary central nervous system lymphoma. *Blood* 117, 1291–1300.
- Szklarczyk, D., Franceschini, A., Wyder, S., Forslund, K., Heller, D., Huerta-Cepas, J., Simonovic, M., Roth, A., Santos, A., Tsafou, K.P., et al., 2015. STRING v10: protein-protein interaction networks, integrated over the tree of life. *Nucleic Acids Res.* 43, D447–D452.
- Tagoug, I., Sauty De Chalou, A., Dumontet, C., 2011. Inhibition of IGF-1 signalling enhances the apoptotic effect of AS602868, an IKK2 inhibitor, in multiple myeloma cell lines. *PLoS One* 6, e22641.
- Takahashi, K., Rochford, C.D.P., Neumann, H., 2005. Clearance of apoptotic neurons without inflammation by microglial triggering receptor expressed on myeloid cells-2. *J. Exp. Med.* 201, 647–657.
- Tan, X., Xu, X., Elkenani, M., Smorag, L., Zechner, U., Nolte, J., Engel, W., Pantakani, D.V.K., 2013. Zfp819, a novel KRAB-zinc finger protein, interacts with KAP1 and functions in genomic integrity maintenance of mouse embryonic stem cells. *Stem Cell Res.* 11, 1045–1059.
- Tayebi, M., Hawke, S., 2006. Antibody-mediated neuronal apoptosis: therapeutic implications for prion diseases. *Immunol. Lett.* 105, 123–126.
- Tayebi, M., David, M., Bate, C., Jones, D., Taylor, W., Morton, R., Pollard, J., Hawke, S., 2010. Epitope-specific anti-prion antibodies upregulate apolipoprotein E and disrupt membrane cholesterol homeostasis. *J. Gen. Virol.* 91, 3105–3115.
- Turk, E., Teplow, D.B., Hood, L.E., Prusiner, S.B., 1988. Purification and properties of the cellular and scrapie hamster prion proteins. *Eur. J. Biochem.* 176, 21–30.
- Wang, J., Lenardo, M.J., 2000. Roles of caspases in apoptosis, development, and cytokine maturation revealed by homozygous gene deficiencies. *J. Cell Sci.* 113 (Pt 5), 753–757.
- Watson, R.W.G., O'Brien, F., Coffey, R.N.T., Fitzpatrick, J.M., 2000. Insulin-like growth factor-1 alters apoptotic signalling in prostate cancer. *Prostate Cancer Prostatic Dis.* 3, S42. S42.
- West, A.K., Hidalgo, J., Eddins, D., Levin, E.D., Aschner, M., 2008. Metallothionein in the central nervous system: roles in protection, regeneration and cognition. *Neurotoxicology* 29, 489–503.
- White, A.R., Everer, P., Tayebi, M., Mushens, R., Linehan, J., Brandner, S., Anstee, D., Collinge, J., Hawke, S., 2003. Monoclonal antibodies inhibit prion replication and delay the development of prion disease. *Nature* 422, 80–83.
- Williamson, R.A., Peretz, D., Pinilla, C., Ball, H., Bastidas, R.B., Rozenshteyn, R., Houghton, R.A., Prusiner, S.B., Burton, D.R., 1998. Mapping the prion protein using recombinant antibodies. *J. Virol.* 72, 9413–9418.
- Wlodkowic, D., Skommer, J., Darzynkiewicz, Z., 2009. Flow cytometry-based apoptosis detection. *Methods Mol. Biol.* 559, 19–32.
- Wu, Y.C., Horvitz, H.R., 1998. C. elegans phagocytosis and cell-migration protein CED-5 is similar to human DOCK180. *Nature* 392, 501–504.
- Wu, B., McDonald, A.J., Markham, K., Rich, C.B., McHugh, K.P., Tatzelt, J., Colby, D.W., Millhauser, G.L., Harris, D.A., 2017. The N-terminus of the prion protein is a toxic effector regulated by the C-terminus. *Elife* 6, e23473.
- Xu, R., Shang, C., Zhao, J., Han, Y., Liu, J., Chen, K., Shi, W., 2014. Knockdown of response gene to complement 32 (RGC32) induces apoptosis and inhibits cell growth, migration, and invasion in human lung cancer cells. *Mol. Cell. Biochem.* 394, 109–118.
- Yang, J., Li, B., He, Q.-Y., 2018. Significance of prohibitin domain family in tumorigenesis and its implication in cancer diagnosis and treatment. *Cell Death Dis.* 9, 580.

- Yao, M., Nguyen, T.-V.V., Pike, C.J., 2005. Beta-amyloid-induced neuronal apoptosis involves c-Jun N-terminal kinase-dependent downregulation of Bcl-w. *J. Neurosci. Off. J. Soc. Neurosci.* 25, 1149–1158.
- Yeo, I.J., Lee, C.-K., Han, S.-B., Yun, J., Hong, J.T., 2019. Roles of chitinase 3-like 1 in the development of cancer, neurodegenerative diseases, and inflammatory diseases. *Pharmacol. Ther.* 203, 107394.
- Yerlikaya, A., Okur, E., Baykal, A.T., Aclan, C., Boyacı, İ., Ulukaya, E., 2015. A proteomic analysis of p53-independent induction of apoptosis by bortezomib in 4T1 breast cancer cell line. *J. Proteomics* 113, 315–325.
- Zafar, S., Behrens, C., Dihazi, H., Schmitz, M., Zerr, I., Schulz-Schaeffer, W.J., Ramljak, S., Asif, A.R., 2017. Cellular prion protein mediates early apoptotic proteome alternation and phospho-modification in human neuroblastoma cells. *Cell Death Dis.* 8, e2557.
- Zambenedetti, P., Giordano, R., Zatta, P., 1998. Metallothioneins are highly expressed in astrocytes and microcapillaries in Alzheimer's disease. *J. Chem. Neuroanat.* 15, 21–26.
- Zhao, Y., Coulson, E.J., Su, X., Zhang, J., Sha, B., Xu, H., Deng, Y., Chen, Y., Cao, J., Wang, Y., et al., 2021. Identification of 14-3-3 epsilon as a regulator of the neural apoptotic pathway for chronic-stress-induced depression. *iScience* 24, 102043.
- Zimmerman, W.C., Sillibourne, J., Rosa, J., Doxsey, S.J., 2004. Mitosis-specific anchoring of gamma tubulin complexes by pericentriol controls spindle organization and mitotic entry. *Mol. Biol. Cell* 15, 3642–3657.